ABSTRACT

EDUCATIONAL LEADERSHIP

CHEN, JUNLI B. E. ZHEJIANG UNIVERSITY, 1987
M. S. SHANGHAI UNIVERSITY OF SCI. & TECH., 1990

CHEMICALLY DERIVED ZIRCONIA TOUGHENED ALUMINA VIA SOL-GEL PROCESSING

Advisor: Dr. Lebone Moeti

Thesis dated May, 1997

Sol-gel processing methods were used to prepare ZTA ceramic powders from high purity materials. The precursor systems used for this research were zirconium butoxide, zirconium isopropoxide, alumium tri-sec butoxide, and yttrium isopropoxide. Other reagents were also used. The emphasis was on mixing the precursor system, performing aging experiments, and heat treatment studies to prepare the final ZTA ceramics.

The effects of processing conditions on the sol to gel transition were examined by varying the water ratios, the ZTA precursor composition and the molar ratio of TEA/alkoxide. It was observed that the TEA/alkoxide molar ratio played an important role in the time for gel formation. The presence of poorly hydrolyzable ligands slows down the

hydrolysis condensation process. The total amount of water for hydrolysis had an effect on the time of gel-formation.

Rheological measurements made during the aging process indicated an increase in viscosity with aging time, which was consistent with changing structure. XRD was used to determine the phase composition after heat treatment. From XRD diagram, alumina is transformed into the α phase after calcination at 1200^0C, the tetragonal ZrO_2 phase was retained on cooling to room temperature in the mixture containing. TG/DTA was also used to deteramine optimum heating schedules. In the presene of zirconia, the alumina phase transformation takes place at a considerably higher temperature than in pure alumina, the more volume percent of ZrO_2, the higher the transformation temperature.

CHEMICALLY DERIVED ZIRCONIA TOUGHENED ALUMINA VIA SOL-GEL PROCESSING

A THESIS

SUBMITTED TO THE FACULTY OF CLARK ATLANTA UNIVERSITY

IN PARTIAL FULFILLMENT OF THE REQUIREMENTS FOR

THE DEGREE OF MASTER OF SCIENCE

BY

JUNLI CHEN

DEPARTMENT OF CHEMISTRY

ATLANTA, GEORGIA.

MAY, 1997

R= viii T= 80

ACKNOWLEDGMENTS

The sincerest appreciation goes to Dr. Moeti, my advisor, for his professional leadership and exceptional patience in all aspects during this study. I would sincerely like to thank the committee members, Dr. Xiu R. (James) Bu and Dr. Yi Pang. I am very grateful to Dr. Karikari for his enriching discussion. I also greatly appreciate the support provided by NASA-FAR and HIPPAC center.

Finally, I would like to dedicate this work to my husband, Yudong Pang, his family and my parents for their immeasurable love and support through my education years.

TABLE OF CONTENTS

ACKNOWLEDGMENTS.....ii

LIST OF FIGURES.....v

LIST OF TABLES.....vii

LIST OF ABBREVIATIONS.....viii

CHAPTER

1. INTRODUCTION.....1

2. BACKGROUND.....4

Powder processing routes.....4

Acetate route: from commercial Alumina and zirconium acetate

Flame route: commercial Alumina and zirconia prepared in the gas phase

A partial chemical route of ZTA powder processing.....6

Wet chemical synthesis powder.....9

Coprecipitation

The sol-gel processing route

Effect of modification agent triethanolamine(TEA) on gel-formation.....21

Rheology.....23

Steady shear flow behaviors

Viscoelastic behavior

X-ray

3. OBJECTIVES....33

4. EXPERIMENTAL APPROACH....34

ZTA sol preparation....35

Property measurements....38

Characterization techniques....38

5. RESULTS AND DISCUSSION....40

TEA affects gel-formation....40

Sol-gel transition....44

Rheological behavior of sample #1

Rheological behavior of sample #2

Rheological behavior of sample #3

FTIR....57

FTIR of sol-gel transition of ZTA precursor

FTIR of ZTA Precursor powder

X-ray powder diffraction....65

X-ray diffraction with different heated temperature

Effect of ZrO_2 on crystallization of Al_2O_3

Thermal analysis....72

6. CONCLUSIONS....75

REFERENCES....77

LIST OF FIGURES

Figure Page

2.1 Mixed powders.....5

2.2 Coprecipitation.....11

2.3A Schematic illustration of nucleophilic polycondensation mechanism of $Zr(OR)_4$.....17

2.3B Schematic illustration of nucleophilic polycondensation mechanism of $Al(OR)_3$.....18

2.3C Schematic illustration of nucleophilic polycondensation mechanism of $Zr(OR)_4$:$Al(OR)_3$.....19

2.4 Schematic illustration of the concept of viscosity under laminar flow.....25

2.5 Schematic plots of (A) shear stress vs. shear rate, and (B) viscosity vs. shear rate for non-Newtonian flow behaviors.....26

2.6 Schematic plots of (A) shear stress vs. shear rate and (B) viscosity vs. shear rate for thixotropic flow behavior.....29

5.1 Stabilization of alkoxide and its hydrolysis.....41

5.2 Plots of viscosity vs. shear rate of ZTA sol #1.....46

5.3 Plots of viscosity vs. shear rate of ZTA gel #1.....47

5.4 Plots of storage modulus, loss modulus, δ vs time of ZTA sol #1.....49

5.5 Plots of storage modulus, loss modulus, and δ vs. time of ZTA gel #1.....50

5.6 Plots of storage modulus, loss modulus, and δ vs. time of ZTA sol #2.....52

5.7 Plots of storage modulus, loss modulus, and δ vs. time of ZTA gel #2.....53

5.8 Plots of storage modulus, loss modulus, and complex viscosity vs. frequency of ZTA sol #2.....55

5.9 Plots of storage modulus, loss modulus, and complex viscosity vs. frequency of ZTA gel #2.....56

5.10 Plots of shear stress vs. shear rate of ZTA sol #3.....58

5.11 Plots of viscosity vs. shear rate of ZTA sol #3.....59

5.12 FTIR of ZTA sol and gel.....60

5.13 FTIR of ZTA sol with and without yttria.....62

5.14 FTIR of ZTA powder.....63

5.15 FTIR of ZTA powder calcined at 1100^0C 66

5.16 X-ray of ZTA powder calcined at 300^0C 67

5.17 X-ray of ZTA powder calcined at 900^0C 68

5.18A X-ray of ZTA powder (Al_2O_3 =93%, ZrO_2 =7%) calcined at 1200^0C 70

5.18B X-ray of ZTA powder (Al_2O_3 =85%, ZrO_2 =15%) calcined at 1200^0C 71

5.19 DTA and TGA curves of ZTA dried gel 73

LIST OF TABLES

Table Page

2.1 Different chemical processes for the preparation of multicomponent oxide systems....10

4.1 Compositions of ZTA ceramics prepared....36

4.2 Initial ATSB, ZRP, YIP volume ratio....37

5.1 Derivatives of alkoxide and its hydrolysis....42

5.2 Effect of synthesis conditions on gelation time....43

5.3 Compositions of three sols....45

LIST OF ABBREVIATIONS

ATSB	Alumium tri-sec-butoxide
DTA	Differential thermal analysis
FTIR	Fourier transform-infrared
h	hour
s	second
TEA	Triethanolamine
TG	Thermal gravimetric analysis
XRD	X-ray diffraction
YIP	Yttrium isopropoxide
ZRP	Zirconium-propoxide
ZTA	Zirconia-toughened Alumina

CHAPTER 1

INTRODUCTION

Tetragonal zirconia (ZrO_2)-toughened alumina (Al_2O_3) has become an area of increased technical interest in recent years [1-3] . By the introduction of dispersed ZrO_2 into an alumina matrix the resulting zirconia-toughened alumina (ZTA) has demonstrated improved toughness and strength when compared to pure alumina [4] . The sliding wear resistance of ZTA ceramics [5] have shown improved properties when compared to Al_2O_3 or tetragonal ZrO_2 ceramics.

Stress induced tetragonal-to-monoclinic(t→m) phase transformation and the stress induced microcracking [6-8] are the principal toughening mechanisms in ZTA ceramics. The stable structure of pure ZrO_2 at laboratory temperature is monoclinic. It transforms to tetragonal symmetry at about 1373 K and transforms back to monoclinic phase with large hysteresis and in a manner characteristic of martensitic transformations[9]. This transformation is unique, since the monoclinic phase has a lower density and has been the key factor [10,11] in the application of stabilized ZrO_2 and ZrO_2 containing ceramic composites as tough materials. The tetragonal phase is stabilized by making solid solutions

with a number of oxides such as MgO, CaO, Y_2O_3, CeO_2, and other rare earth oxides [6,12]. Phase stability is also controlled by particle size since extremely fine particles of ZrO_2 are stable in their tetragonal or even cubic structure at laboratory temperatures [7]. This stability is simply a consequence of the trade-off of unfavorable bulk free energy differences for a favorable surface free energy difference between the two phases [8,13], although recent studies of this transformation in other materials show that the stability of the phases depends upon the strain energies [14,15] and kinetic factors [16,17]. For a purely sol-gel derived powder the absence of a rigid matrix makes the strain terms less likely to influence the transformation. Several studies of the evolution of tetragonal and monoclinic structures in particulates of ZrO_2 obtained by different methods including sol-gel techniques have been reported [18,19]. Crystallite size studies [20-23] have been done both as a function of temperature and isothermal holding times. In brief, such studies have indicated that at higher temperatures the crystallite sizes of the tetragonal phase increase while their numbers decrease and above certain critical sizes, typically about 300A in linear dimension, tetragonal ZrO_2 transforms to the monoclinic [20]. Since control of the initial particle sizes can be achieved by the sol-gel route, it is both interesting and important to examine the evolution of structures in partially stabilized zirconia compositions. Factors such as particle size, particle size distribution, and the nature of the polymorph contribute to the toughening mechanisms and strenghth enhancement. These factors can be modified by the processing techniques used in the fabrication of ZTA ceramics.

It is known that the methods of powder preparation and control of the starting materials, that is, grain size and size distribution, have a direct effect on the material properties. Most of the research conducted in the development of ZTA ceramics has been either by colloidal/powder processing [24] or by partial chemical routes [25]. The disadvantages of these methods include the impurities in the starting materials and the difficulty in achieving good uniform distribution of the zirconia dispersed in the alumina matrix.

In this research, a chemically based approach using high purity starting materials such as zirconium and alumium metal alkoxides was used to control the precursor chemistry and particle sizes and also achieve improved uniform distributions of ZrO_2 dispersed in the Al_2O_3 matrix. By carefully controlling the precursor chemistry, high purity ZTA ceramics with smaller grain sizes can be prepared which should improve the toughness and wear erosion properties of the ZTA ceramics.

CHAPTER 2

BACKGROUND

Toughening of alumina through dispersion of zirconia particles is known to be strongly dependent on the grain size of both species and the quality of the microstructure. In zirconia-toughened alumina (ZTA) the martensitic transformation of zirconia (tetragonal→monoclinic) during the cooling step of sintering is at the origin of toughening. If the zirconia particles have small grain sizes, they remain tetragonal. Grain coarsening of alumina should be limited by the zirconia particles by remain at the grain boundary.

2.1 Powder Processing Routes

The quality of the dispersion during the powder processing is of major importance. When starting from commercial alumina and zirconia, an attrition milling of a well-dispersed slip has been shown to give the best result [26-28]. Using different precursors to prepare ZTA will result in different microstructures and mechanical properties. In the

present study, different precursor routes, or non-commercial powders, have been studied. Different precursor routes exhibit strong differences in the microstructure. This is not only due to the grain size distribution but also to chemical mechanisms in conjunction with grain growth mechanisms.

Figure 2.1 Mixed Powders

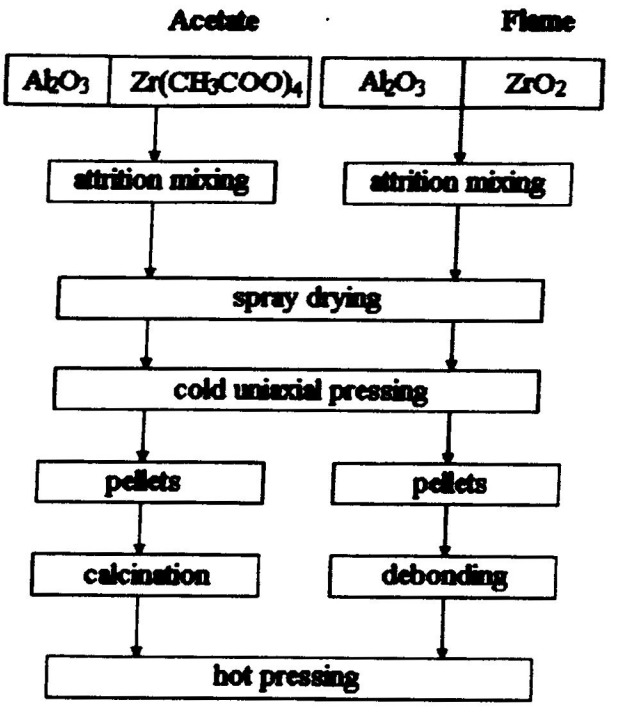

2.1.1 Acetate route: from commercial Alumina and zirconium acetate [29]

Alumina powder is slowly added to zirconium acetate solution(Magnesium Elektron, pH 3). A 6h attrition milling allows a convenient impregnation of alumina

particles by the zirconium salt. The mixture is then spray dried, thus transforming the zirconium acetate into a zirconium hydrate. Cold-pressed powders pellets are then heated in air using a slow temperature increase rate to 900^0C, thus transforming the hydrate into ZrO_2.

2.1.2 Flame route: commercial alumina and zirconia prepared in the gas phase [30,31]

Zirconia powders are prepared by injection of $ZrCl_4$ in a hydrogen-oxygen flame; different specific surfaces may be obtained for zirconia. A Bayer alumina powder and the zirconia powder are optimally dispersed in separate slurries at pH 10 using a dispersant agent [44, 45, 51] and mixed. The resulting slip with a dry matter content of 60% is then spray dried in order to give [10-30] μm spherical agglomerates which are uniaxially pressed and debonded before final hot pressing.

2.2 A partial chemical route of ZTA powder processing

Colloidal/powder processing techniques or partial chemical routes have been used in the development of ZTA ceramics. A partial chemical route using zirconium salt solutions containing Al_2O_3 dispersions is a modification of a powder processing. In this technique, commercially available Al_2O_3 powder containing main impurities of SiO_2, Fe_2O_3, TiO_2, and Na_2O was used. It is widely recognized that the presence of SiO_2 even in very small amounts can lead to glass formation concentrated at the grain boundaries. The

presence of such glass formers lead to reduced strength and toughness at elevated temperature (greater than 1000^0C).

In the development of ZTA, Yttria(Y_2O_3) additions are used to stabilize the ZrO_2 in the tetragonal state. Without the presence of Y_2O_3 to stabilize the zirconia in the tetragonal state, ZrO_2 transforms from tetragonal to monoclinic below 1100^0C. During colloidal/powder processing, Al_2O_3 powders are generally dispersed in a solvent such as methanol and the pH is made acidic by the addition of dilute nitric acid. ZrO_2 is then added in the form of an oxychloride salt solution in a quantity to yield the desired weight percent of ZrO_2 in the final product. Yttrium nitrate, $Y(NO_3)_3$, is also added as the source for Y_2O_3 based on the amount required. The resulting dispersion is then stirred and evaporated to obtain a dry powder. Ball milling of the dry powder followed by calcining at low temperatures is then conducted. The calcined powders is then wet ball milled in a solvent and dried at low temperature. Compacts are then made by cold compaction pressing and the samples are sintered at 1600^0C for two hours in air to obtain the final ZTA ceramic. Using such processing techniques there is very limited control on the particle size and distribution of ZrO_2 in the Al_2O_3 matrix. In addition, the presence of impurities in the starting materials such as SiO_2 can lead, for example, to glass formers at the grain boundaries resulting in reduced high temperature strength and toughness.

Mechanical properties such as hardness, toughness, and elastic modulus will determine to a great extent the wear rate at which material can be removed from a target in addition to the impact conditions(angle of impact, velocity and size of impacting

particles, and the mechanical properties of the erodent). The solid particle erosion properties of tetragonal ZrO_2 (3 mol % Y_2O_3)-toughened Al_2O_3 (ZTA) composities has been investigated for composities prepared from powder processing routes. The mechanical properties of alumina ceramics can be improved by dispersing zirconia in the alumina matrix. The toughening mechanisms associated with zirconia-toughened alumina (ZTA) are related to the phase transformation from metastable tetragonal zirconia to the monoclinic form during cooling after sintering (microcrack toughening) or during mechanical wading (transformation toughening).

High strength and toughness require an optimized transformation-toughening mechanism. This can be achieved by sintering to dense, fine-grained ceramics with zirconia grain sizes less than the critical grain size for spontaneous transformation. A range of wet-chemical techniques have been reported for the preparation of zirconia-alumina ceramic powders which result in fine-grained transition alumina- (γ–, θ–Al_2O_3) containing powders with an intimate mixture of both zirconia and alumina. Transition alumina are metastable and will transform to α-alumina during sintering. The concept of simultaneous sintering and phase transformation was as an alternative processing route for the preparation of alumina ceramics. It is observed a drastic decrease in densification rate upon the phase transformation to α–alumina is a nucleation and growth process

In the investigation where the partial chemical method was used(32), ZTAs with different volume fractions of tetragonal -ZrO_2 were used as the target material. The effects of impact angle and the mechanical properties of the erodent using Al_2O_3 and SiC as

erodent particles was investigated. The optimum wear resistance was determined to be with 7 to 22 vol % tetragonal ZrO_2. The erosion wear properties of the ZTA in terms of wear resistance were better than those of Al_2O_3 or tetragonal ZrO_2 alone in the case of the Al_2O_3 erodent particles. However, in the case of the SiC erodent particles the wear resistance of the ZTA were worse than for the Al_2O_3 or tetragonal-ZrO_2 ceramics.

2.3. Wet chemical synthesis powder

There are various kinds of chemical methods for ceramic powder preparation via the liquid phase, which make it easy to control the properties of the powder product and to prepare fine particles. The chemical processing of ceramics, especially ceramic powder synthesis, has drawn a considerable amount of attention over the past two decades. The reason for this is the demand for reliable and advanced ceramic componets for high-performance applications. A series of typical wet chemical synthesis methods are listed in Table2.1. By means of wet-chemical preparation of ceramic powders, very small crystallites can be obtained with a high degree of homogeneity and improved sinterability. These very fine-grained powders are very difficult to obtain as a really monodispersed powder.The main advantages of these processes are the increased homogeneity and high surface area of the resulting powders which lead to relatively high reactivity and hence low sintering temperatures.

Table 2. 1.Different Chemical Processes for the Preparation of Multicomponent Oxide Systems

1, synthesis from complex precursors

(thermal decomposition):

(a) oxalate route

(b) citrate route

(c) catecholate route

(d) acetate route

2, (a) co-precipitation

(b) freeze-drying

3, evaporative decomposition:

(a) spray pyrolysis

(b) liquid mix process

4, sol-gel processing:

(a) mixed alkoxide route

(b) carboxy-alkoxide route

(c) hydroxide-alkoxide route

5, hydrothermal synthesis

6, gas-phase reactions

(plasma or laser technique)

7, self-propagating combustion

2.3.1.coprecipitation

Figure 2.2 coprecipitation

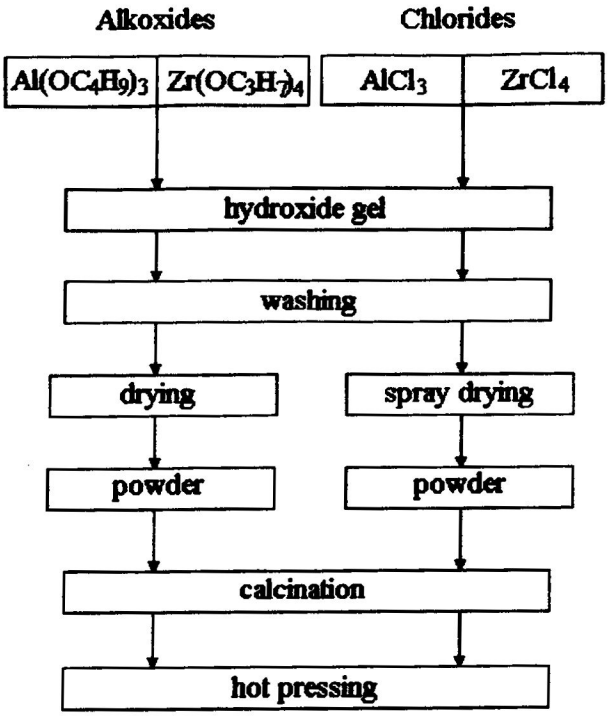

2.3.1.1.Alkoxide route: co-hydrolysis of metallic alkoxides [30,33]

Secondary aluminium butoxide and zirconium(IV) propoxide(Fluka) were dissolved in anhydrous isopropyl alcohol at a concentration of 1.5molL-1. Hydrolysis was carried out by the addition of ammonia(pH 10 or 12) at ambient temperature. The gel was filtered, washed, dried and calcined. The transformation, transition alumina→α-alumina,

takes place at a lower temperature with the powder prepared at pH 10. Alumina is completely transformed into the α phase after calcination at 1200^{0}C. The mean grain size of the powder prepared at pH 10 is much larger than that of the powder prepared at pH 12: grinding is then necessary to obtain a finer grain size.

2.3.1.2 Chloride route: from aluminium and zirconium chlorides [30,34]

A mixture of the aluminium and zirconium oxides is prepared starting from the metal chlorides. An aqueous solution of aluminium ($AlCl_3.6H_2O$) and zirconium ($ZrCl_4$) chlorides is prepared at a concentration of 0.6molL^{-1}. Co-prepicitation of aluminium and zirconium hydroxides is obtained by addition of ammonia at ambient temperature. The gel is washed, dried in an oven and calcinated at 1200^{0}C. The zirconium hydroxide is amorphous; the aluminium hydroxides depending on neutralization pH.

2.3.2 The sol-gel processing route

Sol-gel processing is the most widely employed route and involves a colloidal sol that is converted into a gel through aging. The gel is subsequently calcined, giving rise to a crystalline product. The powder characteristics, such as particle size, particle shape, crystallinity, phase content, surface area and purity, are mostly dependent on the conditions of calcination. The sol-gel process for making ceramics, glasses, and composites has received considerable attention. Investigations on processing and physical properties are voluminous; viscosity measurements have been used to identity certain

points during the sol-gel transition at which sols are suitable for various processing operations, this has practial significance in that sol-gel forming operations may be carried out over a wide range of shear rate conditions.

Sol-gel technology involves the synthesis of inorganic oxides from inorganic or organometallic precursors (usually metal alkoxides). The advantages offered by the use of sol-gel techniques are briefly stated as follows:

1. better homogenity compared to traditional mixed powder technology.
2. high purity compared to mineral raw material sources;
3. lower temperature processing and consolidation is possible;
4. more uniform phase distribution in multicomponent system;
5. easy preparation of thin films and coatings;
6. better size and morphological control in powder synthesis;
7. opportunities for the preparation of new crystalline and non-crystalline solides.

Sol-gel is a multi-step process involving chemical and physical processes associated with hydrolysis, polymerization, drying and densification. The process owes its name to the distinctive rapid viscosity increase that occurs at a particular point in the sequence of steps. This sudden viscosity increase is a common feature in sol-gel processing and signals the onset of gel formation.

A brief description of the steps typically involved in sol-gel ceramic synthesis is as follows:

1. Hydrolysis: the process may start with a mixture of metal alkoxide and water in solvent
2. Polymerization: condensation reactions occur between adjacent molecules in which H_2O and ROH are eliminated and metal oxide linkages are formed. Polymer networks grow to colloidal dimensions in the liquid. The colloidal dispersion is termed a sol.
3. Gelation: polymer networks link up to form a 3-D network throughout the liquid. The system becomes rigid, characteristic of a gel. Solvent and the products of condensation reactions, water and alcohol, remain in the pores of the gel. The aggregation of smaller polymer units to the main network continues progressively if the gel is allowed to age.
4. Drying: water and alcohol are removed from the system at moderate temperature ($<100^0$C), leaving a highly hydroxylated metal oxide with some residual organic content. If a high surface area, low bulk density, aerogel powder is the goal, the solvent may be removed supercritically.
5. Dehydration: fairly high temperatures, 400-800^{0}C, are required to drive off the residual residual organics and chemically bound water, yielding a glassy metal oxide with up to 20-30% microporosity.
6. Densification: temperatures typically in excess of 1000^{0}C cause elimination of porosity and formation of a dense metal oxide.

The sol-gel method has been applied not only to the preparation of single phase oxides, but also to the fabrication of the multiphase composite materials. If a homogeneous multicomponent oxide is desired, mutual solubility of the precursor

alkoxides does not guarantee homogeneity in the final product due to their likely difference in hydrolysis and condensation rates.(Special techniques have been devised to maximize condensation reactions between the different alkoxides and minimize self-condensation reactions.)

Little is known about the growth and structure of gels from mixtures of alkoxides. In the case of aluminosilicate gels, there have been a few studies of the growth mechanism by Pouxviel and co-workers [35-38] and Heinrich and co-workers [39,40,41]. Pouxviel and co-workers employed the double alkoxide $(C_4H_9O)_2Al\text{-}O\text{-}Si(OC_2H_5)_3$, which restricted the stoichiometry of their resultant gels to $Al_2O_3.2SiO_2$. Hydrolysis yields small particles by the condensation of aluminum hydroxyl groups. The gel formation is governed by the hydrolysis of the silicon ethoxy groups. In the resultant gels, silicon atoms are mainly bonded to one aluminum atom. In the case of a homogeneous particle structure, one would expect, from stoichiometry, each silicon atom to be bonded to two aluminum atoms (35-38). Heinrich and co-workers used chelated aluminum alkoxides and tetraalkoxysilane in their investigations. Aerogel monoliths as well as xerogel powders with Mullite stoichiometry ($3Al_2O_3.2SiO_2$) were obtained by their synthesis procedure. They found reaction-limited cluster-cluster growth to be the gel-forming mechanism with the hydrolysis of the alkoxysilane as the reaction-limiting step. The influence of the chelating agent on particle formation was shown to be the reduction of the number of available condensation sites [39,40,41].

The alkoxide route is very common in sol-gel processes. The sol-gel process involves two steps: hydrolysis and condensation. In the presence of water, the alkoxides used in this research undergo hydrolysis:

$$Zr(OR)_4+H_2O\rightarrow Zr(OR)_3(OH)+ROH$$

$$Al(OR)_3+H_2O\rightarrow Al(OR)_2(OH)+ROH$$

$$Y(OR)_3+H_2O\rightarrow Y(OR)_2(OH)+ROH$$

Alkoxy groups (-OR) of the alkoxide are replaced by hydroxyl groups (-OH) of the water and alcohol (ROH) is generated. If hydrolysis of alkoxide is carried to completion, hydrolysis is as follows:

$$Zr(OR)_4+4H_2O\rightarrow Zr(OH)_4+4ROH$$

$$Al(OR)_3+3H_2O\rightarrow Al(OH)_3+3ROH$$

$$Y(OR)_3+3H_2O\rightarrow Y(OH)_3+3ROH$$

In addition to hydrolysis, formation of Zr-O-Al bonds can occur simultaneously by a condensation reaction between two hydroxyl groups with the release of a water molecule:

$$Zr(OH)_4+Al(OH)_3\rightarrow (OH)_3Zr\text{-}O\text{-}Al(OH)_2+H_2O$$

$$Zr(OH)_4+Y(OH)_3\rightarrow (OH)_3Zr\text{-}O\text{-}Y(OH)_2+H_2O$$

$$Al(OH)_3+Y(OH)_3\rightarrow (OH)_2Al\text{-}O\text{-}Y(OH)_2+H_2O$$

If condensation is carried to completion, anhydrous metal oxide is formed. The above examples are illustrative. The mechanism of polycondensation in ZTA may be proposed as follows: (Fig.2.3A, 2.3B, 2.3C). In a nucleophilic substitution mechanism, a deprotonated

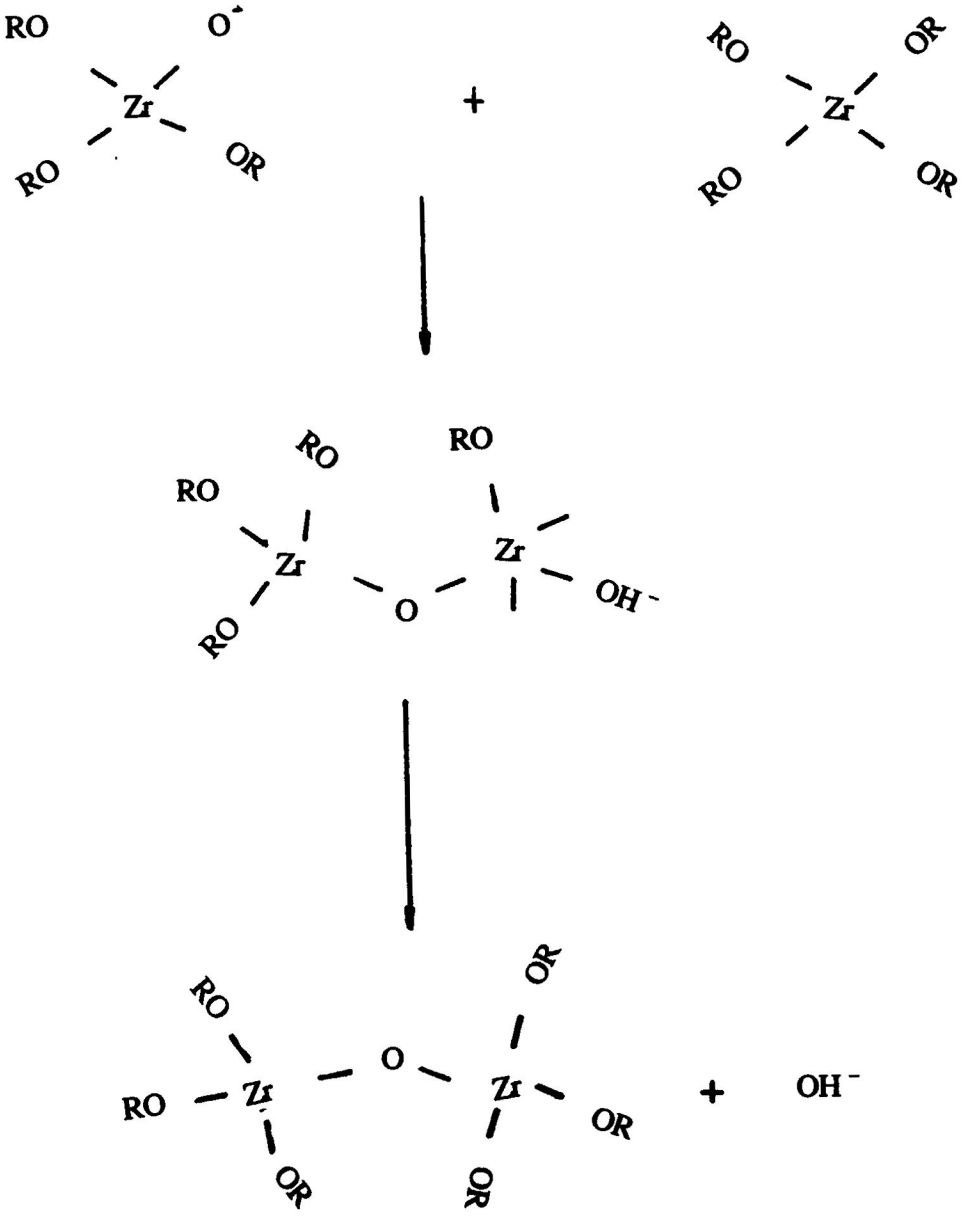

Fig.2.3A Schematic illustration of nucleophilic polycondensation mechanism of $Zr(OR)_4$

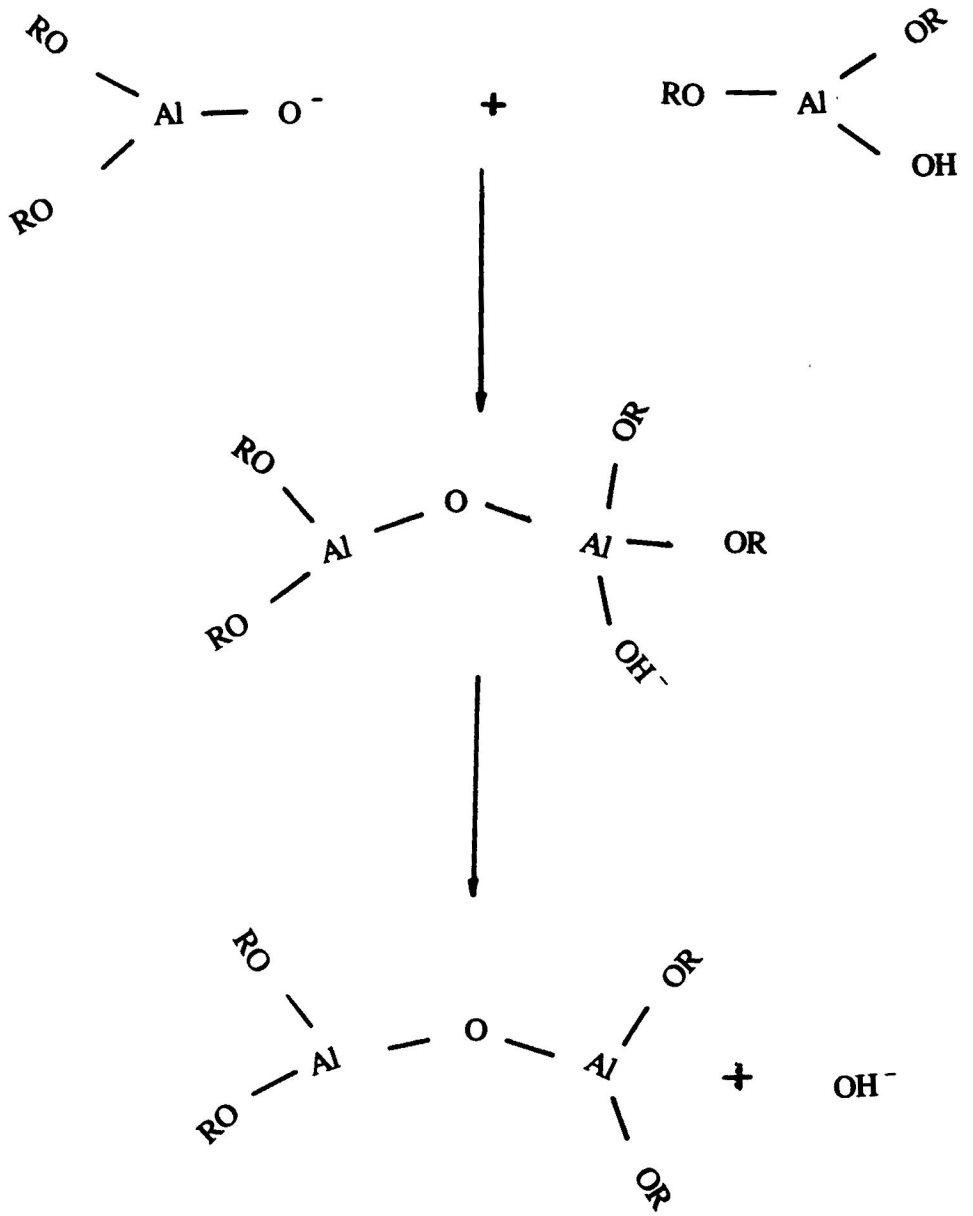

Fig.2.3B Schematic illustration of nucleophilic polycondensation mechanism of $Al(OR)_3$

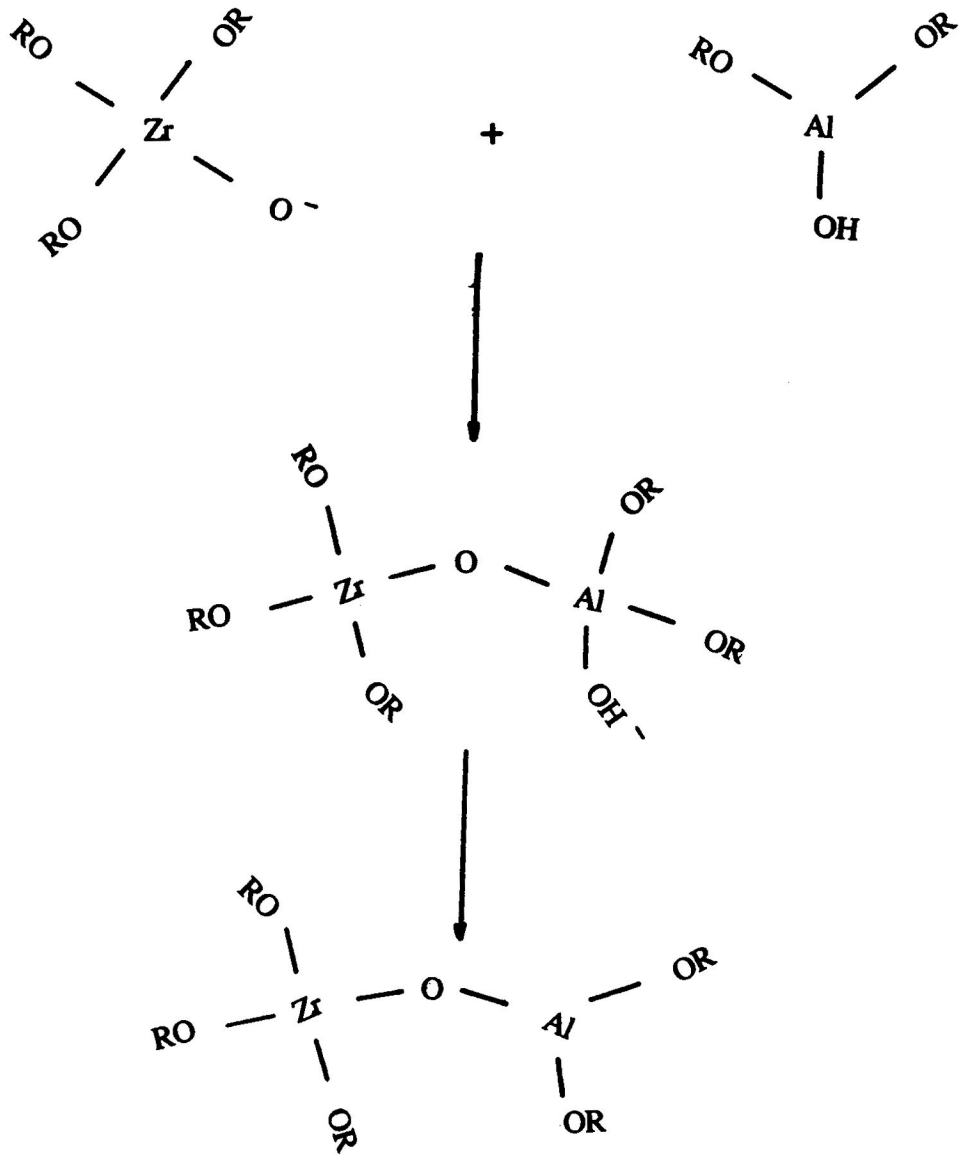

Fig.2.3C Schematic illustration of nucleophilic polycondensation mechanism of $Zr(OR)_4$: $Al(OR)_3$

(M-O-) reacts with a non-ionozed group (M-OH), releasing an OH-. Condensation reactions also occur between partially hydrolyzed (i.e. partially alkoxylated).

In addition to the water concentration, the physical and chemical nature of the metal oxide species depends on factors such as the type and concentration of alcohol and alkoxide. These factors are discussed below. The mixture of metal oxide species in a liquid medium (alcohol/water) is called a "sol" with aging, these species may link up to form a semi-rigid, three-dimensional gel structure.

Initially, the species, which can be either dense colloidal particles or more open "polymeric" species, are dilute and isolated. With aging, continued growth through hydrolysis and polycondensation can occur, but individual species also start to link up and bond together by condensation reactions. With further aging, agglomeration and condensation growth result in the development of the structures with a three-dimensional, network character the so-called "microgel regions". Eventually, the entire sol develops this three-dimensional, network structure, i.e. macroscopic gelation occurs. This "wet gel" can be dried to remove liquids (i.e. alcohol, water) to form a porous aerogel. This aerogel can be densified (i.e. sintered) at higher temperatures to form a dense, final product. Sols prepared with low water content tend to form small, less branched and more chain-like species, with a high water content, sols tend to form species with a greater degree of branching and crosslinking`

Chemistry plays an important role in the sol-gel process. It is complex and in most cases it is difficult to evaluate mechanisms, especially with respect to multicomponent

systems where it is very difficult to separate reactivities of single components but these systems are very often of great practical interest. Chemistry can be used to control important parameters for material tailoring. This "new" chemistry also involves the possibility of incorporating organics into inorganic networks, a class of material which have become of interest in many applications.

The chemical synthesis of inorganic materials has become an important area in materials science. The sol-gel route using metal alkoxides has the possibility of controlling rates of hydrolysis and condensation by chemical means and not by surface or colloid chemistry.The transition from the sol to gel state can be achieved by three different ways:

_ growth of polymeric molecules (which crosslink randomly to a three dimensional network)

_ growth of individual particles (which grow together as they become larger)

_ stabilization of colloids by surface charges(change of the zeta potential and a following interparticular condensation process leads to gelation).

2.4 Effect of modification Agent Triethanolamine(TEA) on gel-formation

The sol-gel transition was characterized by determining the gelation time. Previous results have shown that the gelation time increase as the reactivity of the alkoxide decrease[13], but there is some dependency of the gelation time on the type or amount of chelating agent.The gelation time increases if the amount of TEA employed increases and if the molecular size of the chelating agent is larger. The influence of the

chelating agent on the particle formation manifests itself as the reduction of the number of available condensation sites. The sol-gel process can be appear quite attractive for the preparation of multicomponent systems, since the mixture of various components at a molecular level can be easily achieved in solution. However, the reactivities of metal alkoxides towards hydrolysis are sometime very different and, in these conditions, it is very difficult to build a common network where the various metal ions are included, taking into account the fact the hydrolysis of an alkoxide is easier when the length of its alkoxy chain is shortened. Special procedures were developed to control hydrolysis and condensation. Besides the prehydrolysis of the slower reacting alkoxide, alkoxide chelation of the faster reacting alkoxide is a common procedure employed to avoid local precipitation of faster reacting alkoxide in gels [8]. In general, transition -metal alkoxides (such as Zirconoum-propoxide(ZRP), Yttria isopropoxide(YIP), and Alumium tri-sec-butoxide(ATSB)) are very reactive towards water. Compared with $Si(OR)_4$, the most commonly used type of precursor, whose hydrolysis and gelation is very well studied, the transition-metal alkoxides are different in a number of ways:

1. their lower electronegativity causes them to be more electrophilic and hence more reactive towards hydrolysis and condensation;

2. they have several stable coordination numbers available, thus allowing them to undergo olation, oxolation, alkoxide bridging and other nucleophilic association mechanisms.

The rapid kinetics of nucleophilic reactions has meant studies of hydrolysis and condensation of transition -metal alkoxides are far more difficult than for $Si(OR)_4$ and hence much less is actually known about the specific pathways. However, it is believed that the major pathways for the hydrolysis and condensation reactions of transition-metal alkoxides, in the absence of catalysts, is via nucleophilic substitution. Other organic solvents may react with alkoxides, at least if they contain reactive functional groups capable of nucleophilic attack (functional groups having electronic pairs). Some authors used complexing agents like-diketones, diols, ethers, organic acids, amines, etc. to modify the chemistry of the hydrolysis/condensation reactions. Many of these modifiers allow control over the reactivity of the initial alkoxide in such a way that it is possible to prepare well-defined sol or gel forms. The possibility of modifying the reactivity of the initial precursors by complexation with a modifier is also an advantage in the formation of multi-element oxides.

2.5 Rheology

Rheology is the science which deals with flow and deformation behavior of materials. It describes the deformation and flow of a material under the influence of applied stresses.The rheology response of a fluid is generally expressed as viscosity. The concept of viscous flow may be understood by the following example. Suppose a liquid is confined between two parallel plates of area A separated by a distance, x, as shown in Fig.2.4. A force, F, is applied tangentially to slide the top plate sideways at a velocity, v,

relative to the bottom plate, which is held stationary. Intermediate liquid layers also move in a sideways direction. The top layer moves with the smallest velocity (i.e.zero)(Fig.2.4). However, the velocity gradient dv/dx (or shear rate, γ) is constant

$$\gamma = dv/dx \qquad (1)$$

The shear stress, τ, acting on the top plate, is given by:

$$\tau = F/A \qquad (2)$$

The viscosity, η, is defined as the ratio of shear stress to shear rate:

$$\eta = \tau/\gamma \qquad (3)$$

The units of η are poises when τ is in dyne/cm^2 and γ is in inverse seconds (s^{-1}):

If τ is in Newtons/m^2 (Pascals, Pa) and γ is in s^{-1}, then η is in Pa.s, which is equal to 10 poise: 1 Pa.s = 10 poise

2.5.1 Steady Shear Flow Behaviors (Shear Stress vs. Shear Rate Flow Curves)

2.5.1.1 Newtonian Flow

Newtonian flow behavior (see Fig.2.5.) is characterized by the absence of a yield stress and a linear relationship between shear stress and shear rate (i.e. the viscosity is constant over a wide range of shear rates). Many liquids, solutions, and dilute suspensions show Newtonian flow behavior.

The rate of energy dissipation in a flowing liquid determines its viscosity. With the presence of particles, the rate of energy dissipation is increased, as a result of increased

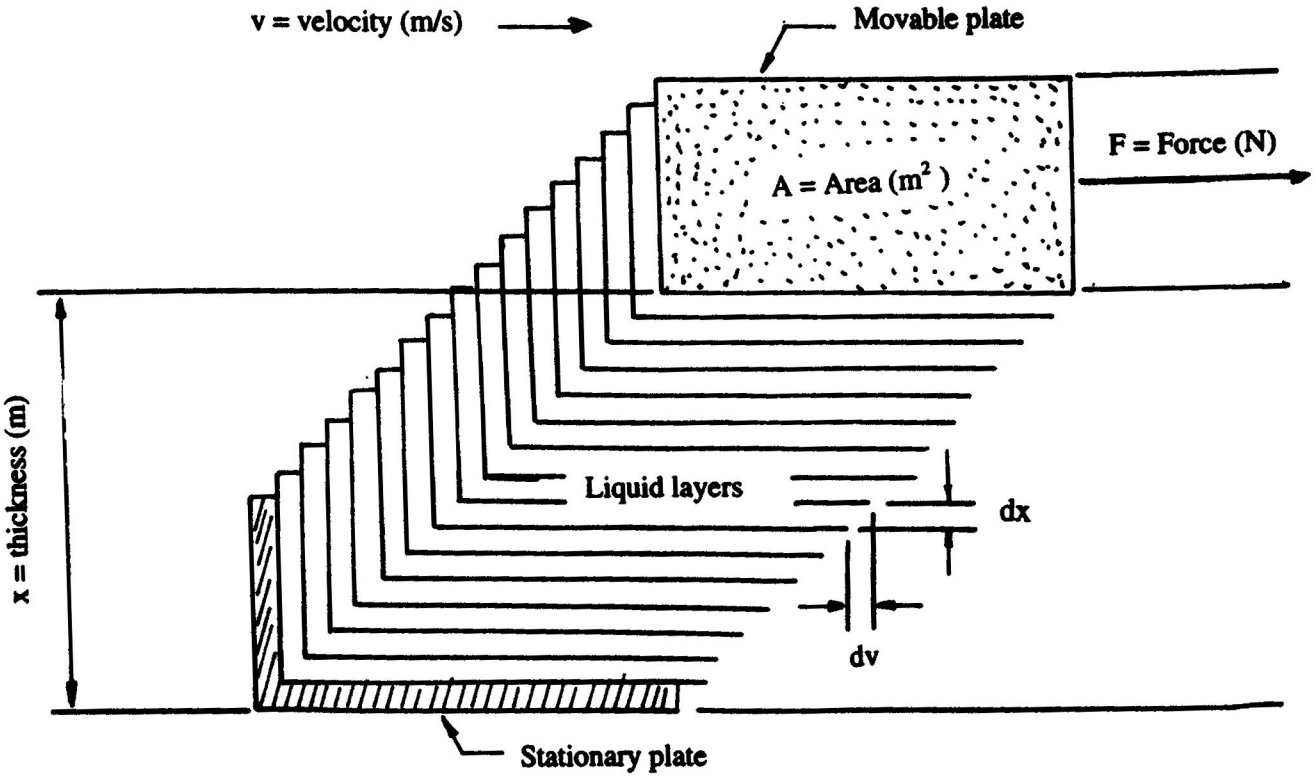

Fig.2.4 Schematic illustration of the concept of viscosity under laminar flow.

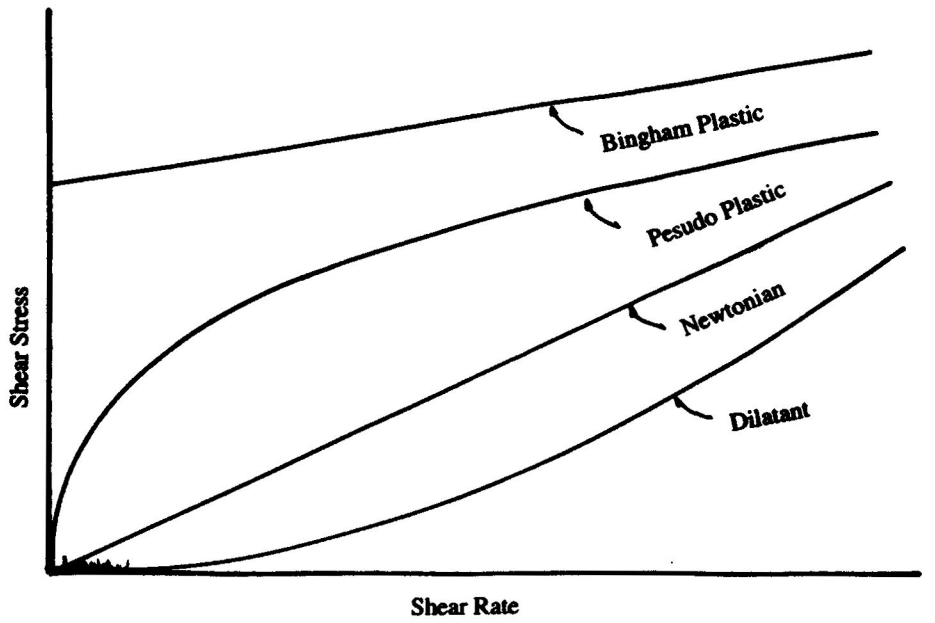

(A)

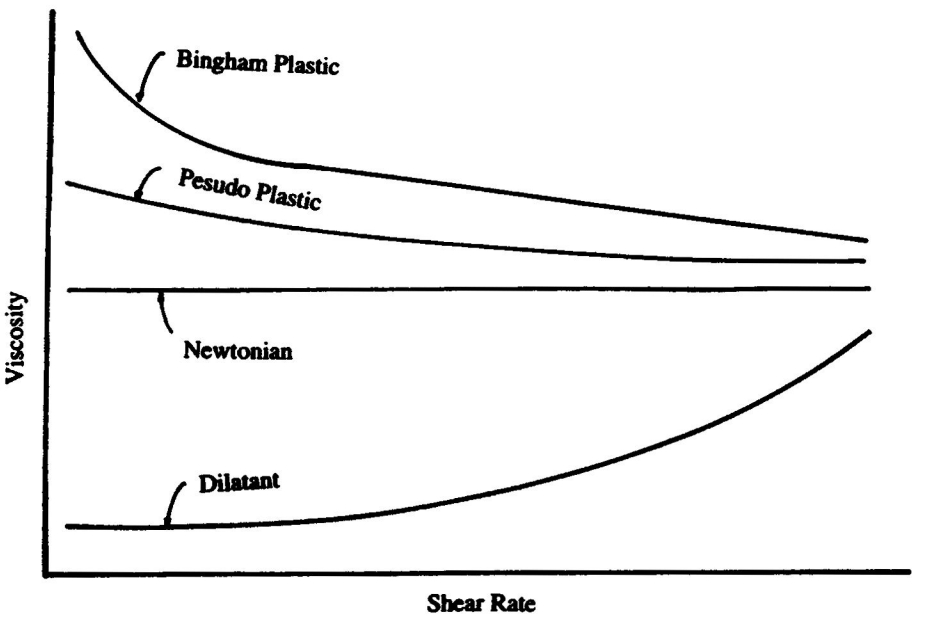

(B)

Fig.2.5 Schematic plots of (A) shear stress vs. shear rate, and (B) viscosity vs. shear rate for non-Nowtonian flow behaviors

perturbations of the liquid streamlines. Therefore, in order to maintain a certain value of shear rate, a larger shear stress is required for a suspension (compared to the particle-free liquid).

2.5.1.2 Non-Newtonian Flow

Non-Newtonian flow behaviors are characteized by the observation of a yield stress and/or non-linear relationships between shear stress and shear rate (see Fig. 2.5A), i.e. viscosity changes with shear rate (see Fig. 2.5.B). Typically types of non-Newtonian flow behavior are described below.

(1) Pseudoplastic Flow (Shear Thinning). In pseudoplastic flow, the slope of the shear stress vs. shear rate curve decreases with increasing shear rate). The change in shear stress and corresponding viscosity are plotted as a function of shear rate in Figs. 2.5A and 2.5B. Shear thinning flow behavior can arise in a number of ways, but thixotropic flow and rheopectic flow are more common than others.

(2) Thixotropic Flow. In discussing the above rheological flow behaviors, it was implied that the flow behavior would be the same by either measuring viscosity with ascending shear rate ("up curve") or by measuring viscosity with descending shear rate ("down curve"). For any given shear stress, there is only one associated shear rate, and, also, for any given shear rate, only one shear stress is observed. However, in some cases, flow behavior may be dependent upon shear history (i.e. previous shear rates, time of shear, etc.). The "up curve" and the "down curve" may not coincide, but instead form a

hysteresis loop (Fig.2.6A). In Fig. 2.6B, the viscosity decreases as the shear rate is increased (the "up curve"). When the shear rate is decreased from its maximum value (the "down curve"), the viscosity (at a given shear rate) is lower than in the "up curve, " indicating that the structure broken down during the period of increasing shear rate is not completely recovered when the shear rate is decreased. The structure may recover with time, although the breakdown also can be irreversible. Rheological flow behavior which shows shear thinning and time dependent behavior is called thixotropic flow behavior. This behavior is indicative of highly structured systems.

2.5.2. Viscoelastic Behavior

It is well known that perfectly viscous liquids behave in according with Newton's law, where shear stress is proportional to shear rate:

Newton's Law: $\tau = \eta.\gamma$

In contrast, perfectly elastic solids behave according to Hooke's law, where shear stress is proportional to shear strain:

Hooke's Law: $\tau = G.\gamma$

where

G = shear modulus

γ = shear strain

Real materials are neither ideally viscous or ideally elastic, i.e. they are viscoelastic. Dynamic, or oscillatory, flow measurements may be used to assess the relative magnitudes

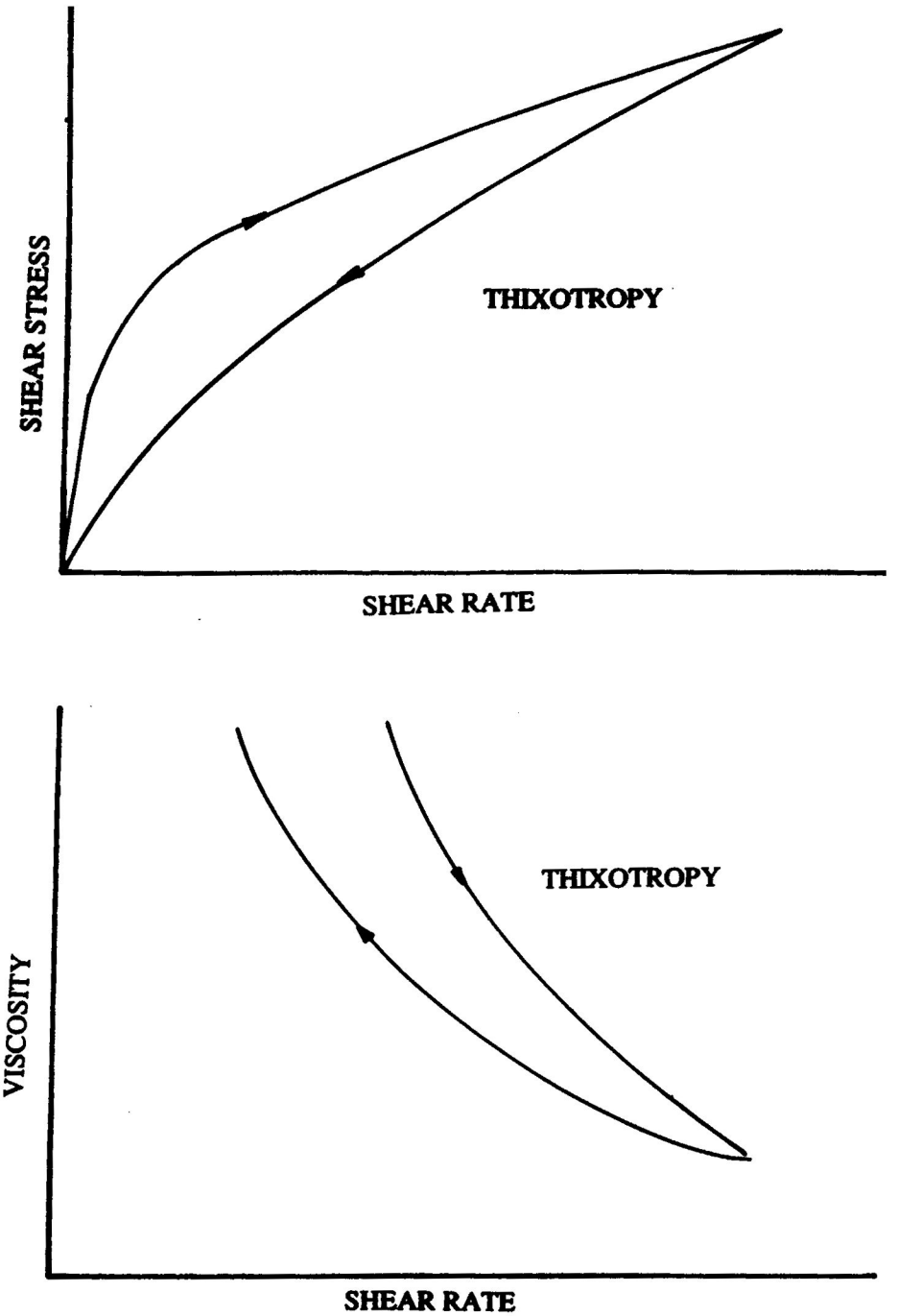

Fig.2.6 Schematic plots of (A) shear stress vs.shear rate and (B) viscosity vs. shear rate for thixotropic flow behavior

of the viscous and elastic character.

$G^* = \tau(t)/\gamma(t)$

$\eta^* = \tau(\tau)/\gamma(\tau) = G^*/i\omega$

where

shear stress: $\tau(t) = \tau_o \exp(i\omega t+\delta)$

shear strain: $\gamma(t)= \gamma_o \exp(i\omega t)$

shear rate: $\gamma(t)=d\gamma(t)/dt = i\omega\gamma(t)$

maximum shear stress: τ_o

maximum shear strain: γ_o

imaginary number $i= (-1)^{1/2}$

$G^* = .G' + iG''$

$G' = |G^*|.\cos\delta$

$G'' = |G^*|.\sin\delta$

$\eta^* = \eta' - i\eta''$

The storage modulus, G', is defined as the ratio of the stress in phase with the strain (in a sinusoidal deformation) to the strain. It represents the energy stored and recovered per cycle of sinusoidal deformation (i.e. it is indicative of the elastic character of the material). The loss modulus, G", is defined as the ratio of stress 90^0 out of phase with

strain to the strain. It represents the energy dissipated or lost, in terms of heat, per cycle of sinusoidal deformation (i.e. it is indicative of the viscous character of the material). The loss tangent, tan δ, is defined as the ratio of the loss modulus to storage modulus:

$$\tan \delta = G''/G'$$

The dynamic viscosity, η', is defined as the ratio of stress in phase with shear rate to shear rate . It is the real part of complex viscosity.

$$\eta' = |\eta^*|.\sin \delta = G''/\omega$$

These parameters are very useful in assessing structural characteristics of solid/liquid systems. A small storage modulus indicates that structure is not extensive (i.e. particle-particle interactions are not significant). On the other hand, a larger storage modulus is observed with more highly structured systems in which particle-particle interactions and the development of three-dimentional networks are important.

Rheologists have long believed that all fluids are viscoelastic in behavior. As a result , the deformation of any fluid from the imposition of a stress is the sum of an elastic deformation, which is recoverable, and viscous flow, which is not recoverable. For fluids of low viscosity at moderate rates of shear, the elastic recovery is extremely rapid and the relaxation time is extremely short. The fluid is considered simply viscous. When viscoelastic fluids are stressed, some of the energy is stored elastically and various parts of the system are deformed into new nonequilibrium positions relative to one another. The remainder of the energy is dissipated as heat and various parts of the system flow into new equilibrium positions relative to one another.

2.6 X-ray

X-ray powder diffraction is the most widely used method for the determination of the phase composition of powders. The angle diffraction of X-rays by the crystalline planes is characteristic of the crystal structure, and the intensity of scattered radiation is characteristic of the atomic composition. In the ZTA powder, phase identification is by X-ray diffraction analysis. 2θ-scans between 27^0 and 33^0 were used to estimate the tetragonal/monoclinic ZrO_2 ratio; 2θ-scans between 55^0 and 62^0were used to confirm either the tetragonal or the cubic ZrO_2 phase.

CHAPTER 3

OBJECTIVES

This research will conduct to synthesis ZTA powders using the sol-gel method and to understand the sol to gel transitions in the ZTA sol-gel precursor systems. The gelation of alkoxide by the sol-gel method was used for the formation of a precursor composed of an alumina-zirconia network structure. The objective of this investigation is to determine the feasibility of sol-gel processes for preparing powders of alumina and phase-stabilized and to establish the relationship between geling condition and the resulting powder properties.

The objectives in this research has included establishing the synthetic conditions required for the preparation of high purity ZTAs. Precursor sols both with and without yttria to stabilize the zirconia have been prepared. Hydrolysis conditions have been established such that sols can be gelled in several hours or several days. Depending on the molar ratio of chemical modified TEA with alkoxide, water content. Characterization techniques used X-ray, rheology, FTIR, thermal analysis.

Chapter 4

Experiment Approach

High purity starting materials were used to synthesize ZTA ceramics with 7, 15, and 22 volume percent of zirconia (i. e. 10, 21, 30 weight percent of zirconia). Aluminum tri-sec butoxide (ATSB), zirconium propoxide, and yttrium isopropoxide were the reagents used. Triethanolamine (TEA) was also used to stabilize the ATSB, ZRP, YIP by the formation of chelating complexes between the ATSB, ZRP, YIP and the TEA which reduced the reactivity of ATSB, ZRP, YIP to water. 2-Butanol was used as solvent in all experiments. Sols both with and without yttria precursor to stabilize the zirconia were prepared. Hydrolysis conditions were established such that sols could be gelled in several hours or days depending on water content and amount of TEA used. The mechanism of sol-gel transformation was examined, the gel structure and its thermal decomposition were investigated. The microstructural evolution of ZrO_2-Al_2O_3 based gels derived from organic precursors is related to the nature of precursors and their processing. Several characterization and analytical techniques have been utilized in this investigation. These

include FTIR, XRD, SEM, and TG/DTA measurements.The precursors of these powders are metal-organic compounds, mainly metal alkoxide. The different compositions of ZTA ceramic powders synthesized by mixed metal alkoxide precursors were the focal points. The chemicals used for preparation of ZTA powder by sol-gel processing are as follows:

1, Alumium tri-sec-butoxide (ATSB)

2, Zirconoum-propoxide solution in 1-propanol (ZRP)

3, Yttria isopropoxide, 25% in toluene (YIP)

4, Triethanolamine (TEA)

5, 2-butanol

6, De-ionized water

4.1 ZTA sol preparation

Table 4.1. shows the composition of ZTA ceramics prepared in this research using the sol-gel approach.

Table 4.1 Compositions of ZTA Ceramics Prepared

	ZrO_2	Al_2O_3	Y_2O_3
	volume%	volume%	mol%ZrO_2
formula # 1	7	93	0
formula # 2	7	93	3
formula # 3	7	93	6
formula # 4	7	93	9
formula # 5	15	85	0
formula # 6	15	85	3
formula # 7	15	85	6
formula # 8	15	85	9
formula # 9	22	78	0
formula # 10	22	78	3
formula # 11	22	78	6
formula # 12	22	78	9

Table 4.2 Initial ASTB ZRP YIP volume ratio

	ASTB (ml)	ZRP (ml)	YIP (ml)
formula #1	12.49	1.00	0.00
formula #2	12.49	1.00	0.12
formula #3	12.49	1.00	0.24
formula #4	12.49	1.00	0.36
formula #5	5.33	1.00	0.00
formula #6	5.33	1.00	0.12
formula #7	5.33	1.00	0.24
formula #8	5.33	1.00	0.36
formula #9	3.27	1.00	0.00
formula #10	3.27	1.00	0.12
formula #11	3.27	1.00	0.24
formula #12	3.27	1.00	0.36

The alkoxide precursors of Al_2O_3 and ZrO_2 with and without Y_2O_3 were dissolved and mixed in 2-butanol and chemically stabilized using TEA and then hydrolyzed in a controlled manner, so that polymerization reactions between the alkoxides proceed under conditions of continuous mixing with a magnetic stirrer, The solution mixing was done at room temperature. Controlled gelation of the sols were conducted such that gels were

obtained after several hours, several days or several weeks. The gel obtained was then dried in a vaccum oven at 80^0C for one day or longer. These gel pieces were ground with a pestle and mortar at this stage to avoid any further grinding later during heat treatment, thereby avoiding any stress induced tetragonal to monoclinic phase transformation in the powder sample. The dried gel were characterized during the heat treatment process at different temperature 300^0C, 600^0C, 900^0C, 1100^0C, 1200^0C.

4.2 Property Measurements

4.2.1 Rheology Characterization

Rheological properties of the precursor sols and gels were monitored and correlated to the synthesis conditions. Rheological flow characteristics were determined using a concentric cylinder viscometer. Steady rotational flow curves (i.e. shear stress, τ, vs, shear rate, γ)were generated by increasing the shear rate for one minute, immediately followed by decreasing the shear rate for another one minute. The viscosity, η, was determined using the following relation:

$$\eta=\tau/\gamma \qquad (4)$$

4.3 Characterization Techniques

The precursor dry gels were characterized using differential thermal analysis (DTA) and thermogravimetric analysis (TGA). The calcined powders were examied by X-ray diffraction(XRD). FTIR spectroscopy was used to follow the structural evolutions in

the precursor sol to gel transition, The chemical structures of ZTA dry gel were also examined using FTIR . The measurements were made on the samples mixed with KBr at 1:50 weight ratio. For the DTA and TGA, the samples were heated at 10^0C/min in a high-purity Alumina pan and a flowing air atmosphere. For the X-ray diffraction, samples were characterized by a powder X-ray diffractometer using nicked-filtered CuKα radiation. Powder X-ray diffraction (XRD) data were obtained by scanning at a rate of 0.25^0 (2θ) min^{-1}. The crystallinity and microstructure of the final ceramics were examined by XRD Scanning Electron Microscopy (SEM), respectively.

CHAPTER 5

RESULTS AND DISCUSSION

5.1 TEA affects gel-formation

In the case of ZTA systems, hydrolysis of ASTB, ZRP, YIP leads to rapid precipitation due to the high hydrolysis rate of these alkoxide. Such precursors are thus quite difficult to use to prepare multicomponent systems. In this research ASTB, ZRP, YIP modified with TEA were used as precursors to prepare ZTA gels. Chelating ligands slowed the reactivity of the precursor towards water. Gels can easily be obtained, when these alkoxides are modified with TEA. The TEA modification reaction is illustrated as follows:

$$Al(OR)_3 + N(CH_2CH_2OH)_3 \rightarrow N(CH_2CH_2O)_3Al + 3ROH$$

$$3Zr(OR)_4 + 4N(CH_2CH_2OH)_3 \rightarrow [N(CH_2CH_2O)_3]_4Zr + 12ROH$$

$$Y(OR)_3 + N(CH_2CH_2OH)_3 \rightarrow N(CH_2CH_2O)_3Y + 3ROH$$

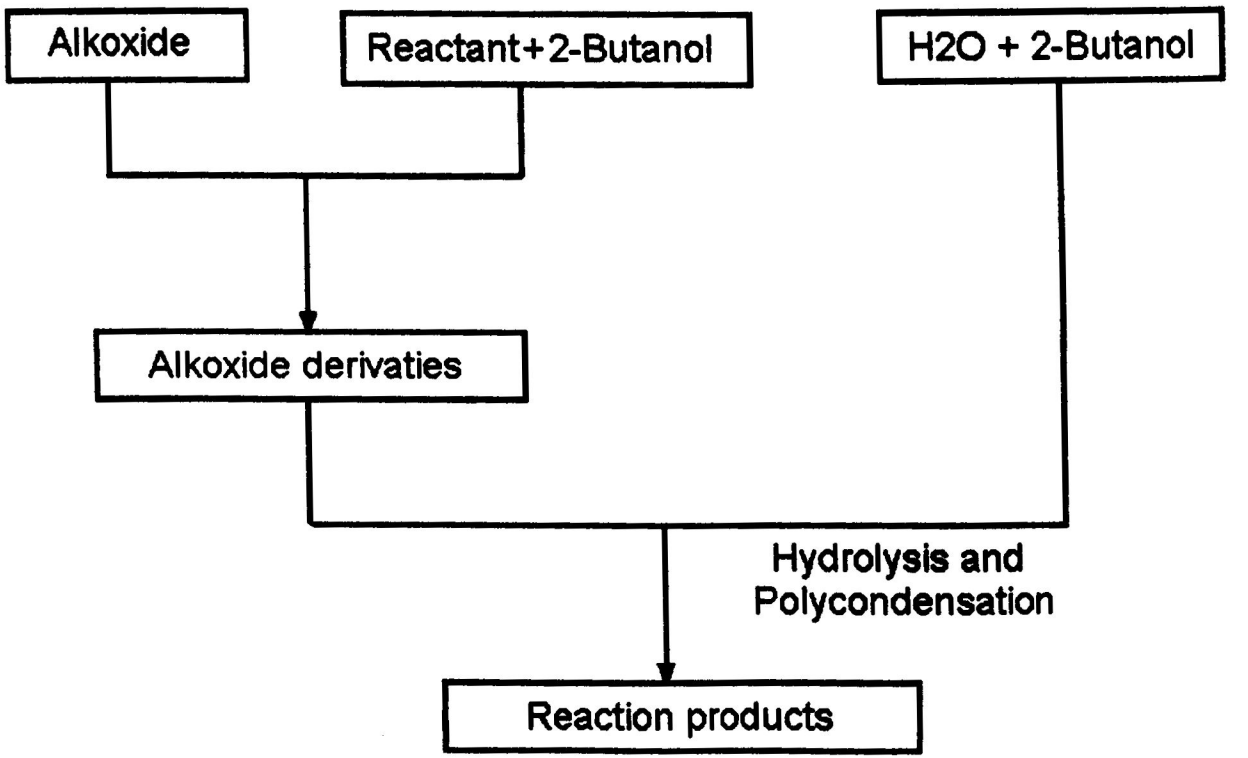

Fig.5.1 Stabilization of alkoxide and its hydrolysis

Table 5.1 Derivatives of alkoxide and its hydrolysi

Reactant	Products	Hydrolysis H_2O/2-BuOh soln
———	Clear soln	Precipitate
$N(CH_2CH_2OH)_3$	Clear soln	Clear soln

Table 5.2 Effect of Synthesis Conditions on Gelation Time

Sample #	ATSB ($molx10^2$)	ZRP ($molx10^3$)	YIP ($molx10^3$)	sec-butanol (ml)	H_2O/Alkoxide (molar ratio)	TEA/Alkoxide (molar ratio)	ZrO_2 (volume %)	Gel Time (hours)
1	4.75	2.23	0.0	30.0	2.0	0.30	7.0	8.
2	6.09	2.86	0.0	40.0	2.0	0.32	7.0	24.0
3	6.09	2.86	0.0	40.0	2.0	0.33	7.0	48.0
4	6.09	6.69	0.0	40.0	2.0	0.33	15.0	10.0
5	6.09	6.69	0.0	40.0	2.0	0.34	15.0	24.0
6	3.81	6.83	0.0	30.0	2.0	0.28	22.0	1.0
7	3.81	6.83	0.0	30.0	2.0	0.30	22.0	6.0
8	3.81	6.83	0.80	30.0	2.0	0.33	22.0	10.0
9	3.81	6.83	0.80	30.0	2.0	0.35	22.0	40.0
10	4.75	2.23	0.0	30.0	4.5	0.35	7.0	0.5
11	6.09	6.69	0.0	40.0	4.5	0.39	15.0	192

The reactivity of alkoxides towards moisture can be modified by chelating ligands TEA. During hydrolysis, butoxy and proxy groups are rapidly removed, but the presence of less hydrolyzable ligands slows down the reactivity of the precursor towards water. Precipitation can be avoided. Thus, this precursor can be used in the preparation of ZTA ceramics. The time for gel-formation depends heavily on the molar ratio of TEA to alkoxide.Table 5.2 show the effect of synthesis on the gelation time.

The rates of hydrolysis of ATSB, ZRP, YIP are somewhat different. At the same molar ratio of TEA/alkoxide and H_2O/alkoxide, the gel-formation of 15% ZrO_2 is faster than the gel-formation of 7% ZrO_2. Water concentration (r = moles H_2O/moles alkoxide) has a significant effect on the structure of the ZTA species, the hydrolysis rate increases as the water concentration increases. Thus, at high water concentration ($r>4$), sols are more completely hydrolysed and, therefore, are more likely to condense with a greater degree of branching and crosslinking. It is only at very low water concentrations ($r\leq2$), sol produces the chain-like, i. e. "polymeric" species.

5.2. Sol-Gel Transition

The first step of the sol-gel process is the transformation of fluid sols to solidified gels, and this step is quite important for the success in this method. Studies of the rheological characteristics of the sol is important in understanding the reactions involved in the sol-gel transition. For instance, rheological characteristics and their time dependence

can provide information on shapes and aggregation states of particles. Also the viscous behavior might give some light on the reaction mechanisms of hydrolysis and polymerization.

The three representative ZTA precursor sol samples were chosen to characterize the rheological properties of the sol to gel transition. The compositions of the three samples are shown in Table 5.3.

Table 5.3 The Composition of the Three Sols Used for Rheological Characterization

sample#	2-but (ml)	ATSB (ml)	ZRP (ml)	YIP (ml)	TEA/alkoxide (molar ratio)	H2O/alkoxide (molar ratio)	ZrO2 volume%
sample#1	40	16	1.28	0.0	0.3458/1	2/1	7
sample#2	40	16	3.0	0.0	0.3327/1	2/1	15
sample#3	40	10	3.06	0.74	0.3384/1	2/1	22

Initially, ZTA precursor sample #1 is dilute with time, though both condensation growth and agglomeration are occuring, The "microgel" regions start to form. Eventually, a three-dimensional network structure is developed. Based on this, certain transitions in rheological flow behavior may be predicted. Initially, very little species-species interaction occurs, (Fig.5.2). The formation of "microgel" regions (Fig.5.2) should result in sols with shear thinning flow behavior, since agglomerates may be broken down, thereby releasing the entrapped liquid and resulting in a lower viscosity. As a more extensive three-dimensional network structure develops (Fig.5.3), a yield stress and hysteresis in the shear

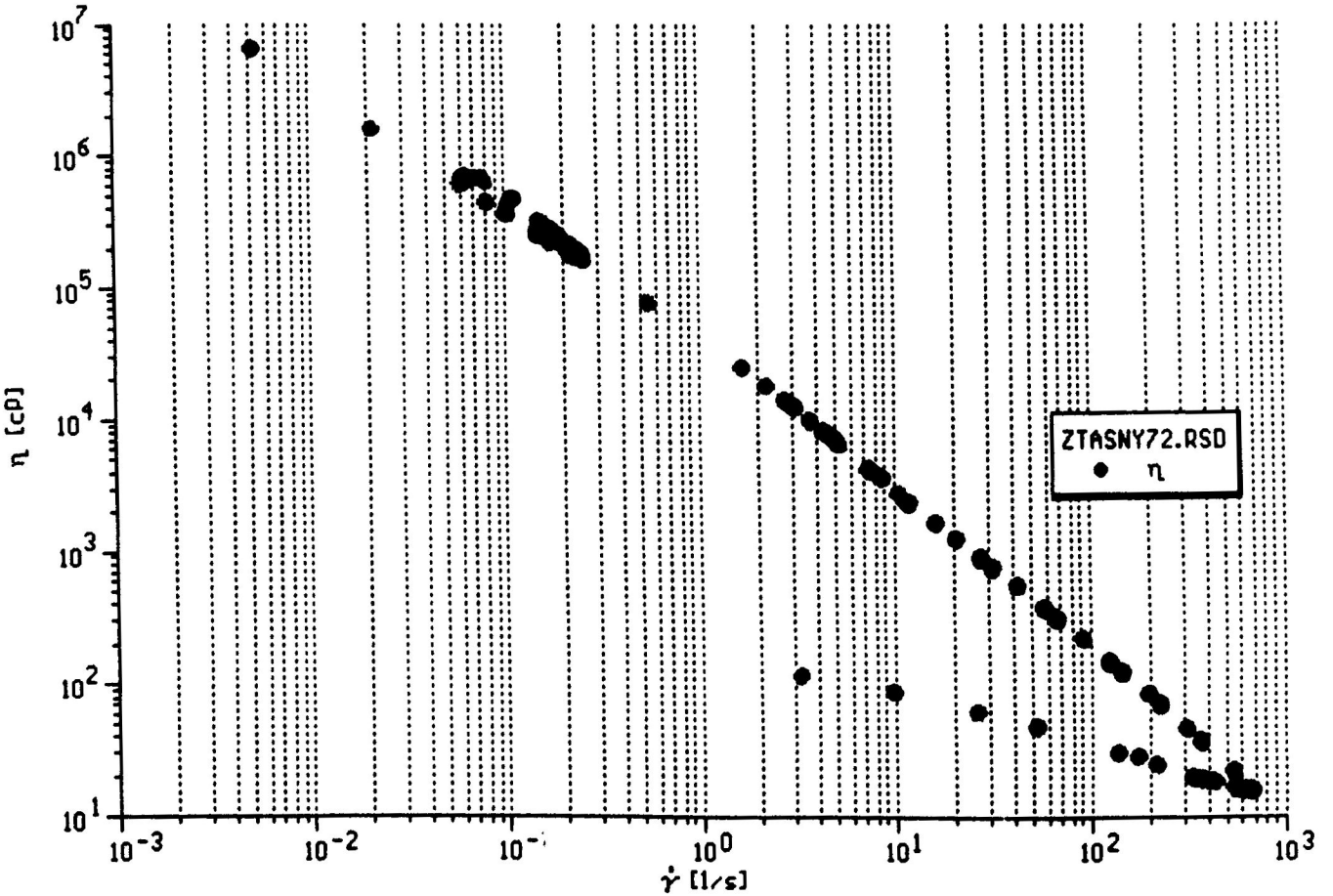

Fig.5.2 Plots of viscosity vs. shear rate of ZTA sol #1

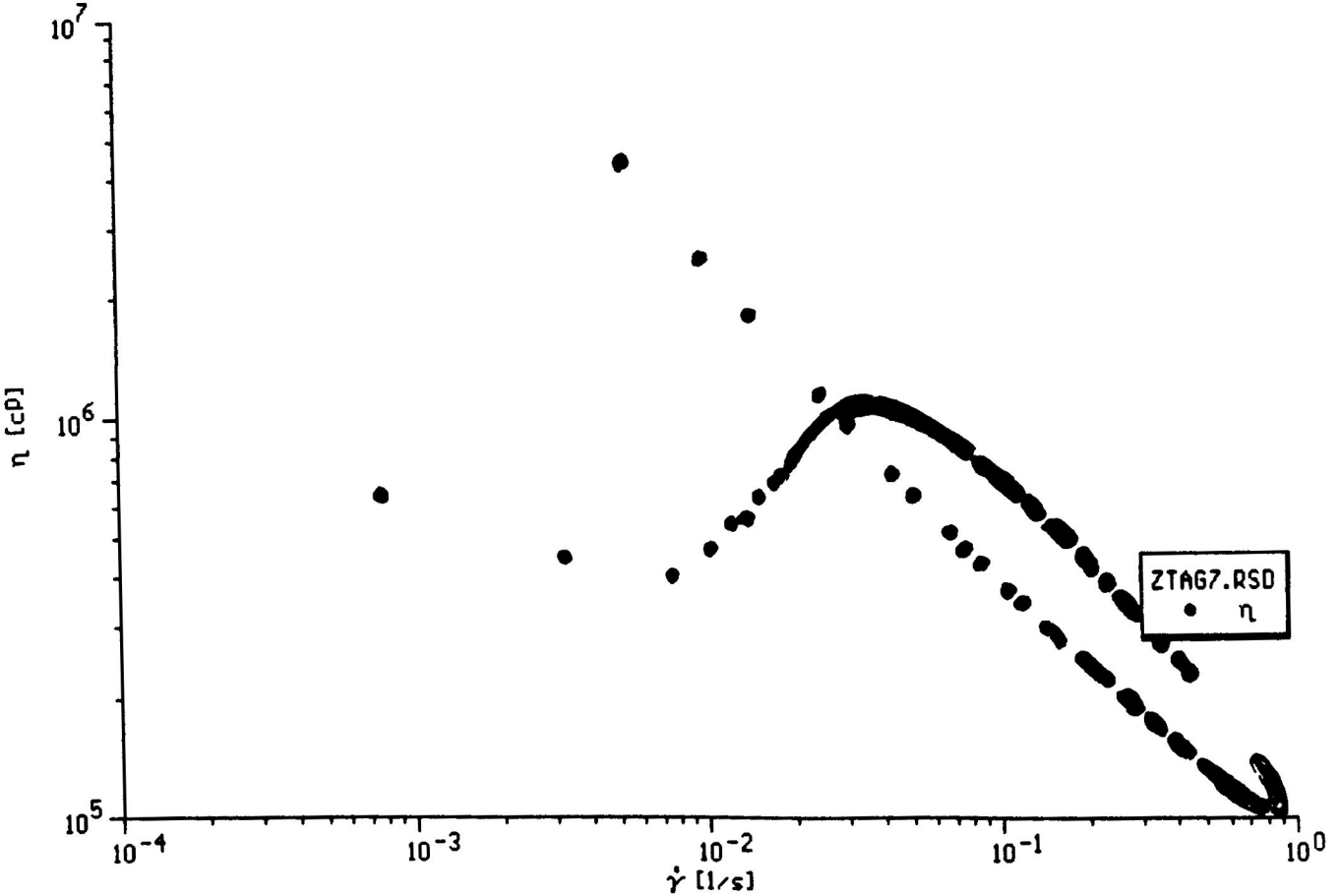

Fig.5.3 Plots of viscosity vs. shear rate of ZTA gel #1

stress vs. shear rate curve (i.e. thixotropy) are expected. As shown below, these transitions in rheological flow behavior are indeed observed during the sol-gel transition.

5.2.1 Rheological Behavior of sample #1

The rheological behavior of sol #1 is discussed below, which includes: (1) viscosity change during aging, (2) shear stress vs.shear rate flow curves, and (3) viscoelastic properties.

5.2.1.1 Viscosity Change

As observed in Fig.5.2, viscosites decrease with an increasing shear rate, i.e. shear thinning behavior is observed in the later stages of the sol state.

5.2.1.2 Viscoelastic properties

The structural changes that occur due to the condensation growth and agglomeration of sol species are also reflected in measurements of the viscoelastic properties during the sol-gel aging period. Plots of the storage modulus (G') and the loss modulus (G"), δ vs time (t) from initial sol to gel are shown in Fig.5.4, Fig.5.5. for sample #1.

During the sol, the viscous modulus dominates (Fig.5.4.), no elastic modulus is formed. This reflects the minimal particle-particle interactions in the "dilute" sol. Both the storage modulus and the loss modulus increase slowly. However, it is observed from

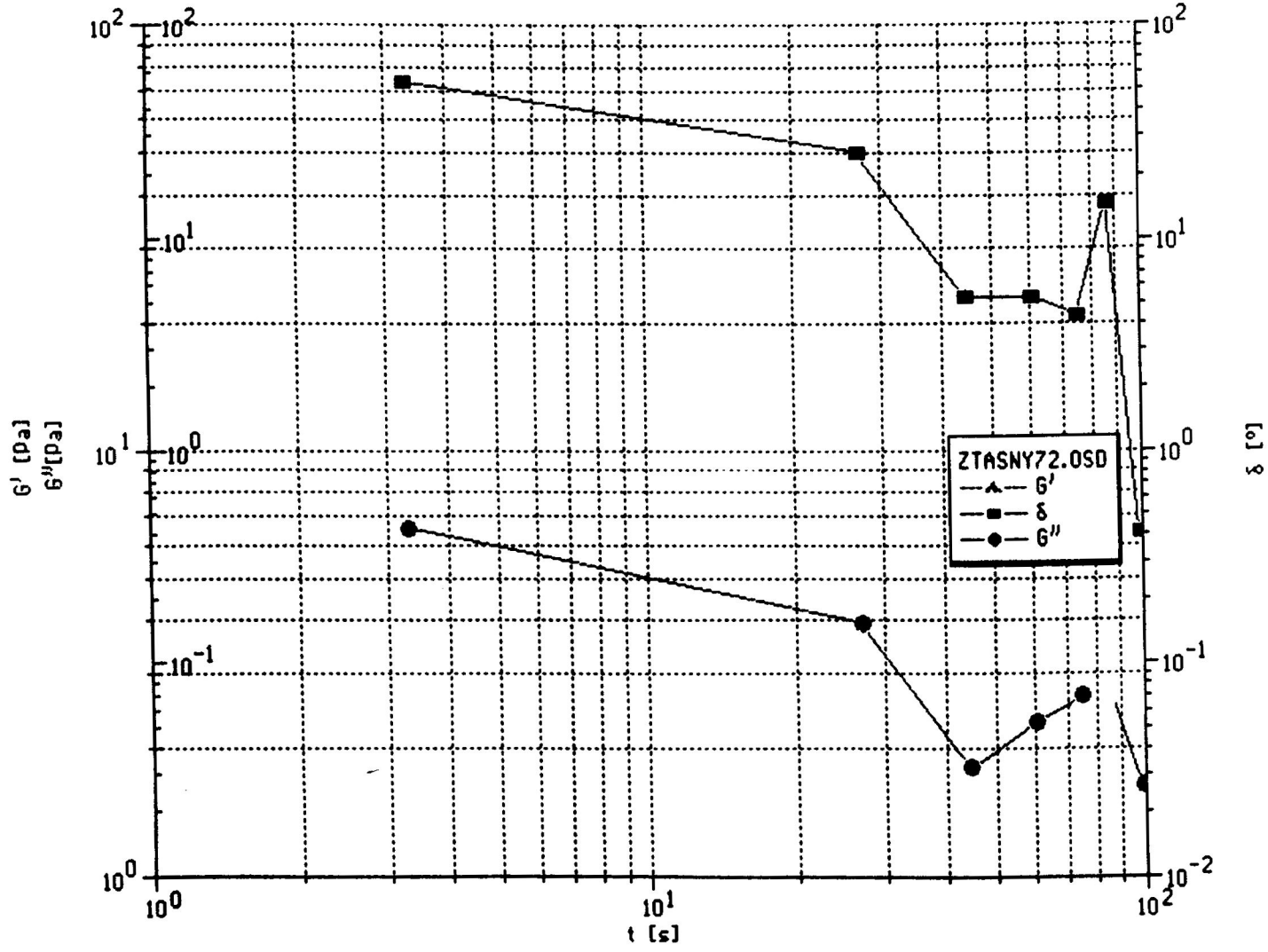

Fig.5.4 Plots of storage modulus, loss modulus, and δ vs. time of ZTA sol #1

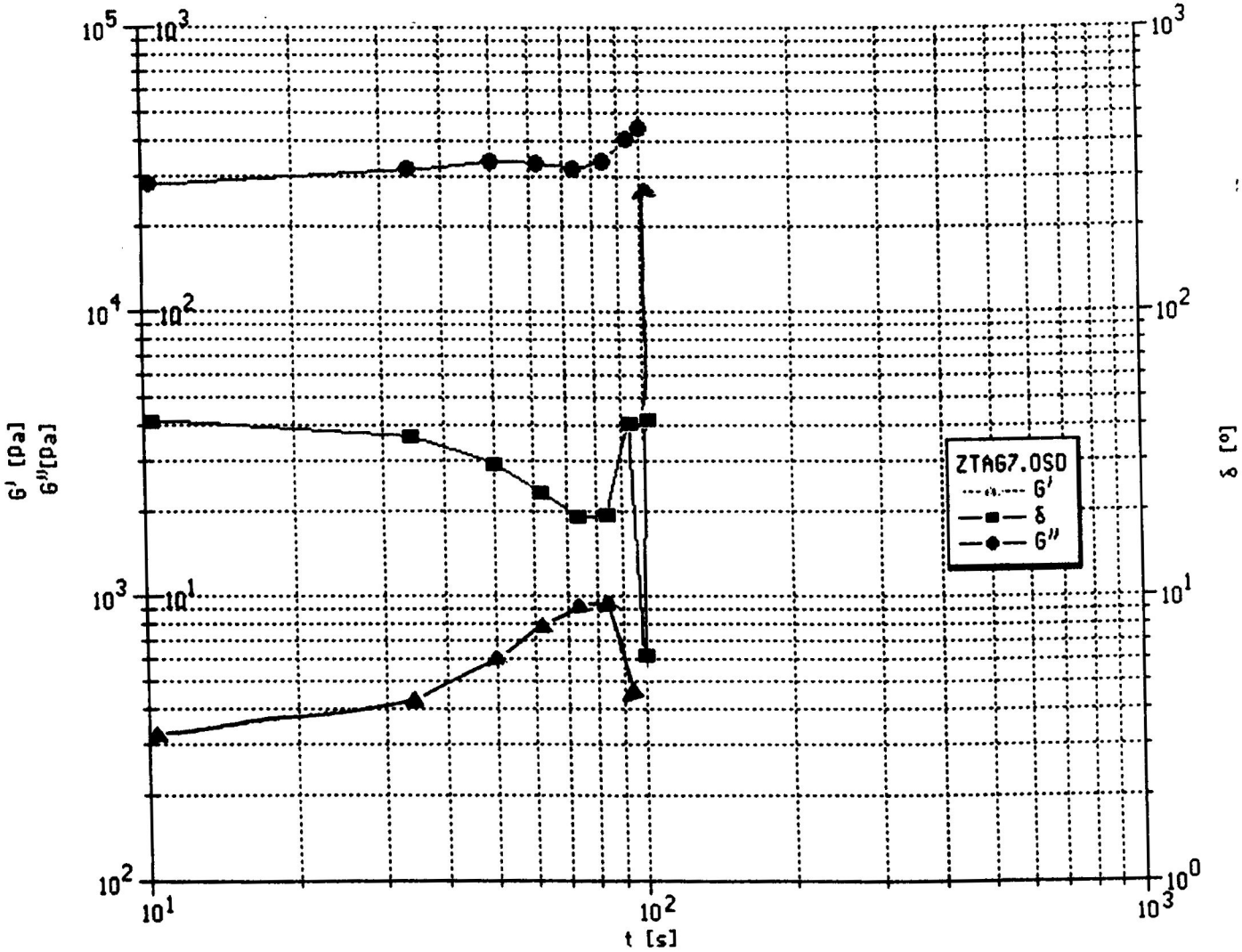

Fig.5.5 Plots of storage modulus, loss modulus, and δ vs. time of ZTA gel #1

(Fig.5.5) that the loss modulus increases more quickly than the storage modulus. The increase in loss modulus G" results in an increased rate of energy dissipation during flow. With further aging, both G' and G" increase quickly. The increase in G' reflects extensive particle-particle interactions and network structure development. The latter effect dominates during the period of shear thinning flow behavior, as indicated by the fact that the storage modulus (G') increases at a faster rate than the loss modulus (G"). Fig.5.4.and Fig.5.5. show the changes in storage modulus, loss modulus, and δ as a function of time (t) for sample #1 at different aging time. In Fig.5.4, G" dominates, G' is not formed over the entire time range examined, in the early stages of aging (Fig.5.4.), the concentration of sol species is relatively low and minimal species-species interactions occur. As indicated by the fact that G">G' over the entire time range measured. The sol behavies similarly to a well-dispersed suspension with low solids loading.

5.3.1 Rheological Behavior of sample #2

Plots of storage modulus, loss modulus and danamic viscosity vs time(t) are shown in Fig.5.6. and Fig.5.7. during the sol, the viscous modulus dominates (Fig.5.6.) no elastic modulus is formed. This reflects the minimal particle-particle interactions in the "dilute" sols. With further aging, both G' and G" increase quickly. The increase in G" reflects the rapid increase in effective solids loading as microgel formation occurs. The increase in G' reflects extensive particle-particle interactions and network structure development. However, it is observed from Fig.5.7. that the storage modulus increases more quickly

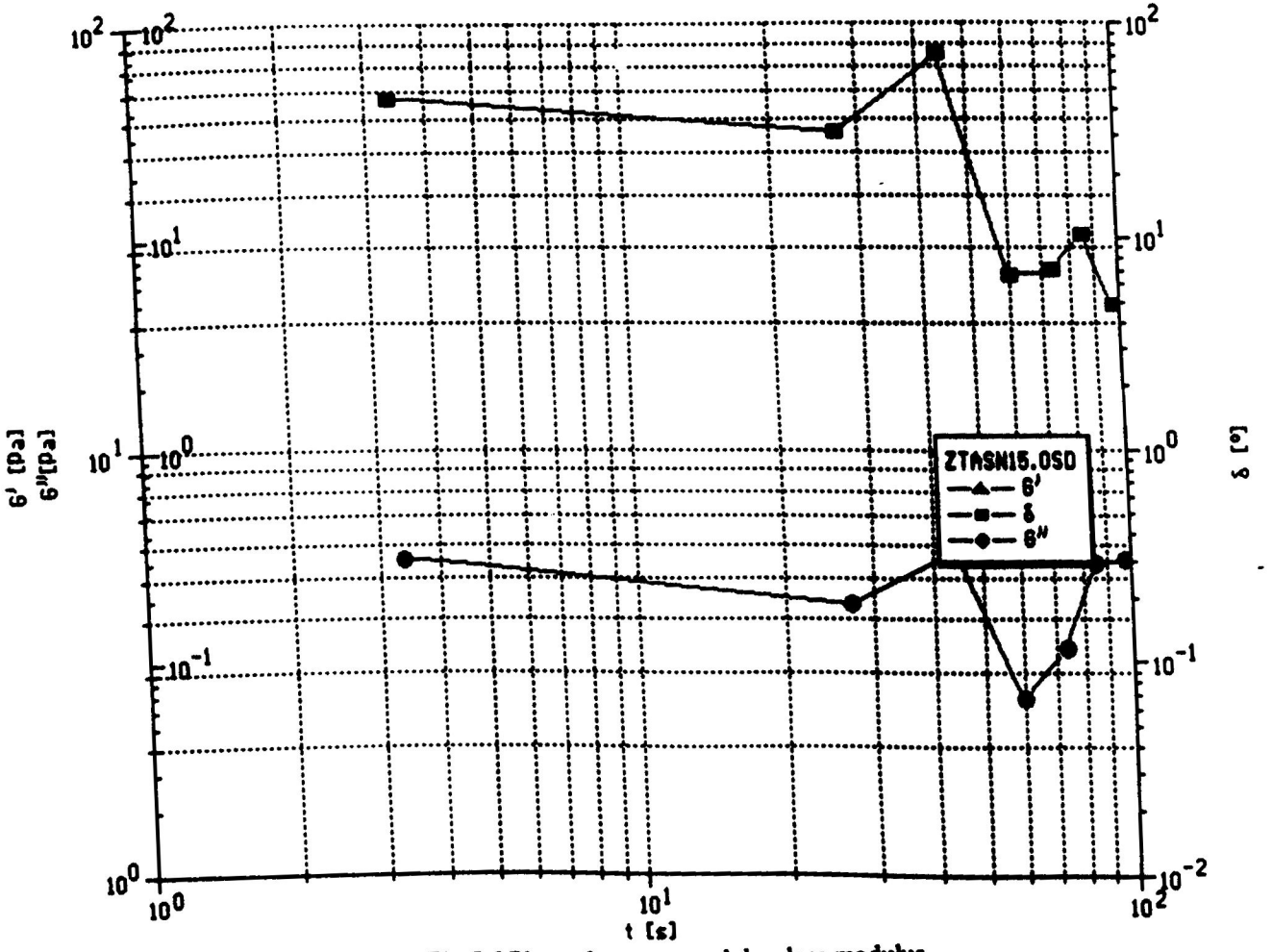

Fig.5.6 Plots of storage modulus, loss modulus, and δ vs. time of ZTA sol #2

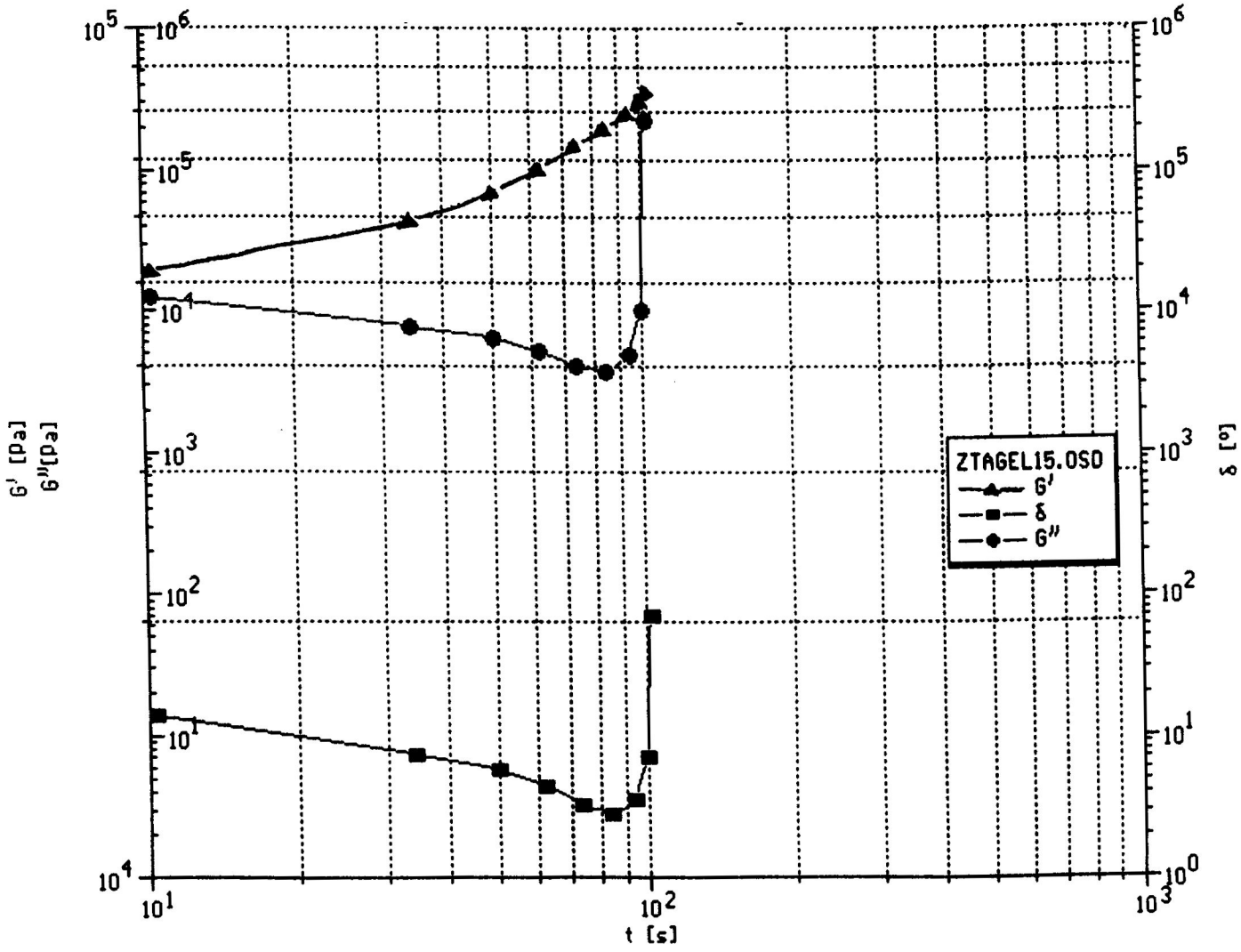

Fig.5.7 Plots of storage modulus, loss modulus, and δ vs. time of ZTA gel #2

With further aging, both G' and G" increase quickly (Fig. 5.9.). The increase in G" reflects the rapid increase in effective solids loading as microgel formation occurs. The increase in G' reflects extensive particle-particle interactions and network structure development. The latter effect dominates during the period of shear thinning flow behavior, as indicated by the fact that the storage modulus (G') increases at a faster rate than the loss modulus (G"). This is clearly seen by the decrease in η^* in Fig.5.9.

The storage modulus increases very rapidly, compared to the increase in the loss modulus (Fig.5.9.), during the thixotropic flow period. The sharp decrease in η^* reflects the rapid development of an extensive , three-dimensional network structure. The large values of G', G", and η^* (i.e. compared to sol in Fig. 5.8.) and the strong angular frequency dependence of the dynamic viscosity indicate that effective solids loading of the sol is high and that the species-species interactions are extensive. The larger values of the elastic modulus (relative to the loss modulus) also reflect the importance of the network structure.

5.4.1. Rheological Behavior of sample #3

For sample #3, during the later stages, viscosity is dependent on shear rate and shear thinning behavior is observed. Plots of shear stress vs. shear rate and viscosity vs. shear rate are shown in Fig.5.10 and Fig.5.11, respectively. As aging proceeds, there is continued condensation growth and agglomeration of sol species. As large agglomerates, i.e. "microgel" regions form, at low shear rates, these "microgel" regions result in high sol

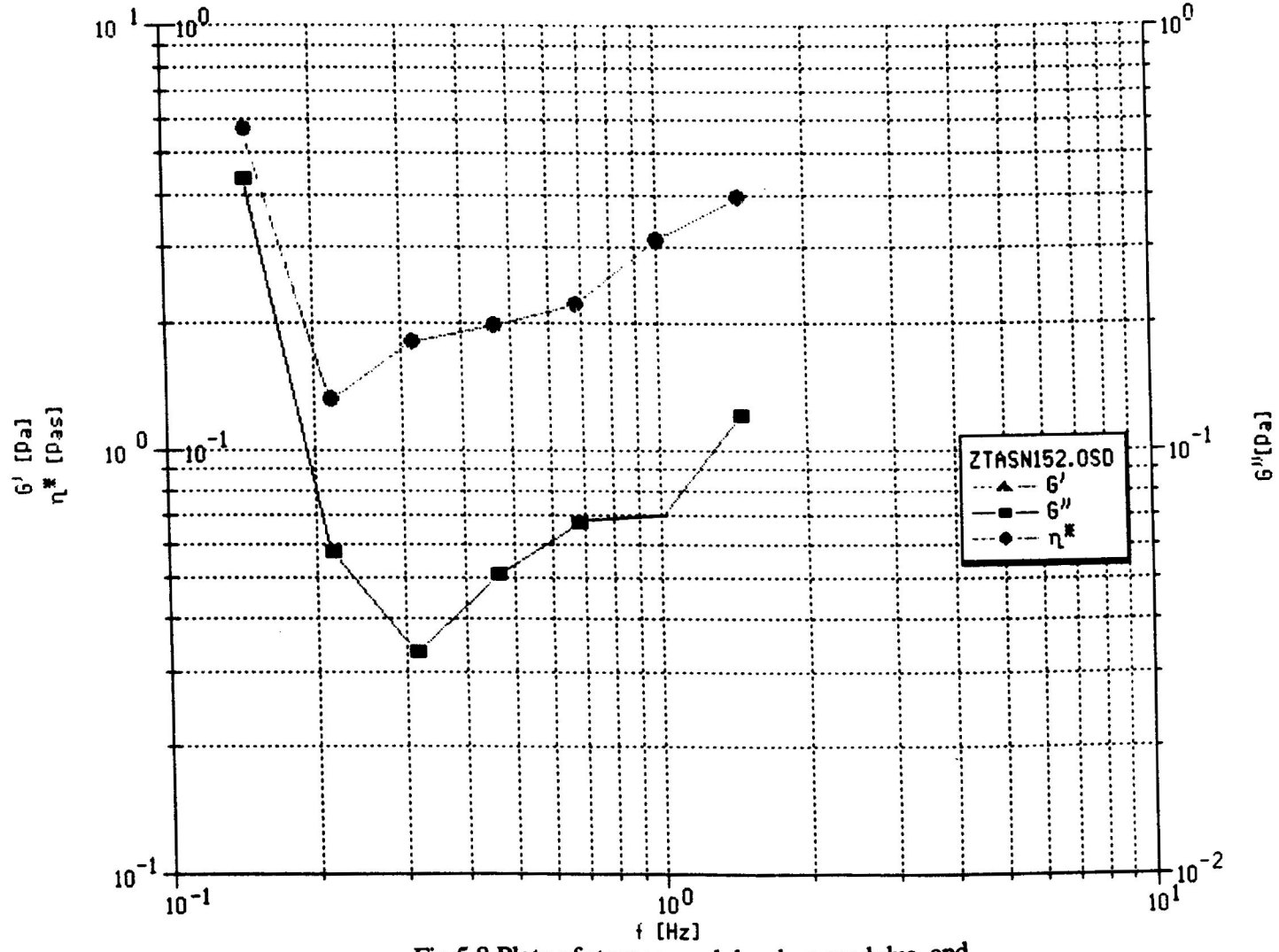

Fig.5.8 Plots of storage modulus, loss modulus, and complex viscosity vs. frequency of ZTA sol #2

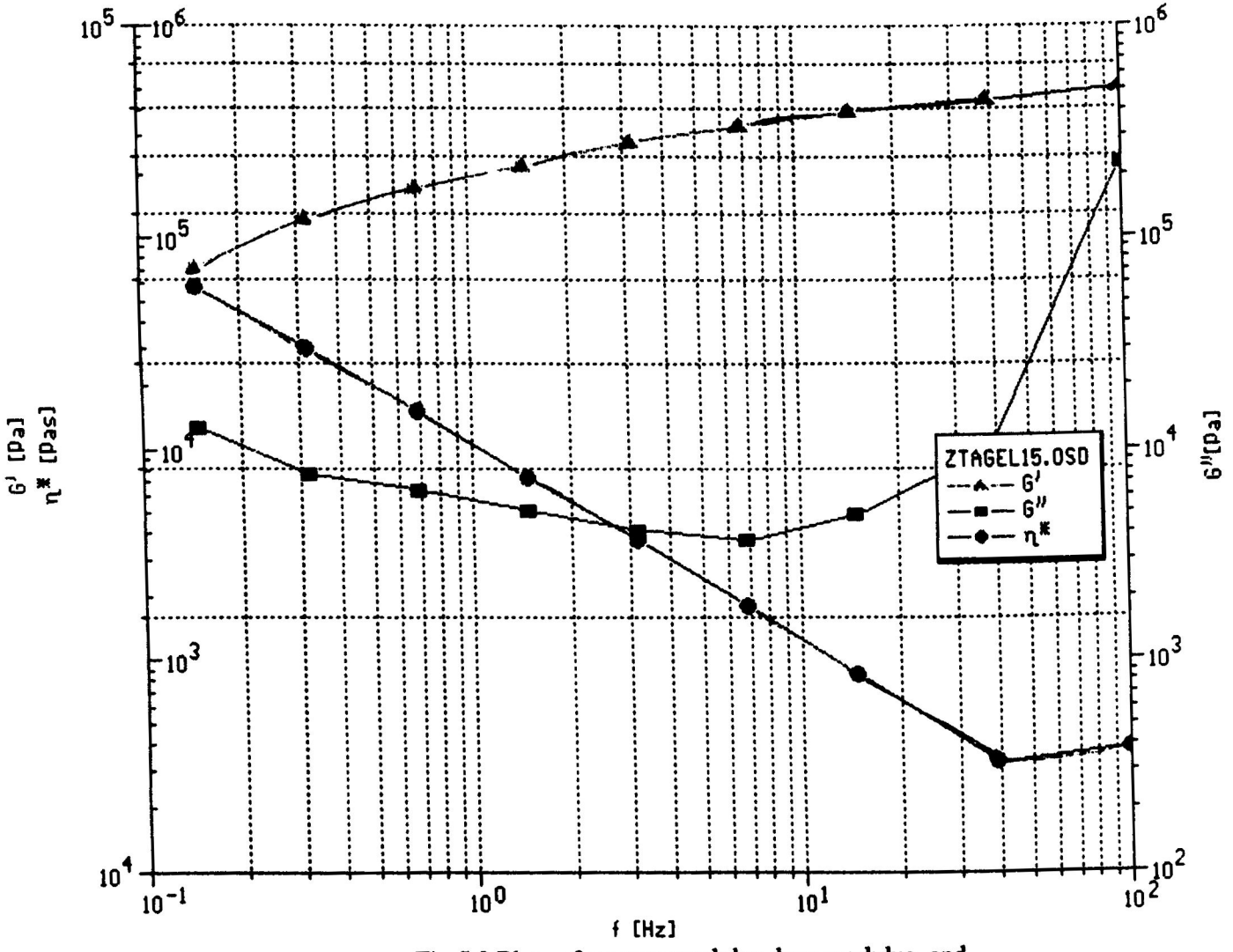

Fig.5.9 Plots of storage modulus, loss modulus, and complex viscosity vs. frequency of ZTA gel #2

visosities. In Fig.5.10. the up curve does not coincide with the down curve, a hysteresis loop is formed, the viscosity decreases as the shear rate is increased (the "up curve"), agglomerate breakdown occurs, releasing immobilized liquid and resulting in lower viscosities. This indicates that particle-particle interactions and the development of three-dimentional networks are important.

Samples #1-3 show similar rheological behavior in both steady and dynamic flow. Although differences in chemical composition produce species with different structure, each sol still undergoes a similar increase in viscosity and similar transitions. Each sol also undergoes similar changes in G', G", and η. There are, however, some differences between the various sols.It is obvious that differences in the gelling rate exists. The gelling process is controlled by many factors, such as water concentration, sol composition, TEA/alkoxide molar ratio, etc. The rapid gelling rate is attributed primarily to the higher H_2O/alkoxide molar ratios, the lower water content leads to a slower hydrolysis rate.

5.5. FTIR

5.5.1. FTIR of Sol-Gel Transition of ZTA Precursors

Fig.5.12 show the FTIR spectra of a ZTA sol and gel, respectively, the sol-gel transition depends heavily on the concentration of TEA. The samples sol of Fig.5.12A and gel Fig.5.12B are the same composition except with different TEA concentrations, with yttria precursor after 2 hours of aging. The greater extent of hydrolysis of the gel in comparision to the sol is observed by the larger peak at 3450cm^{-1} wave numbers. This is

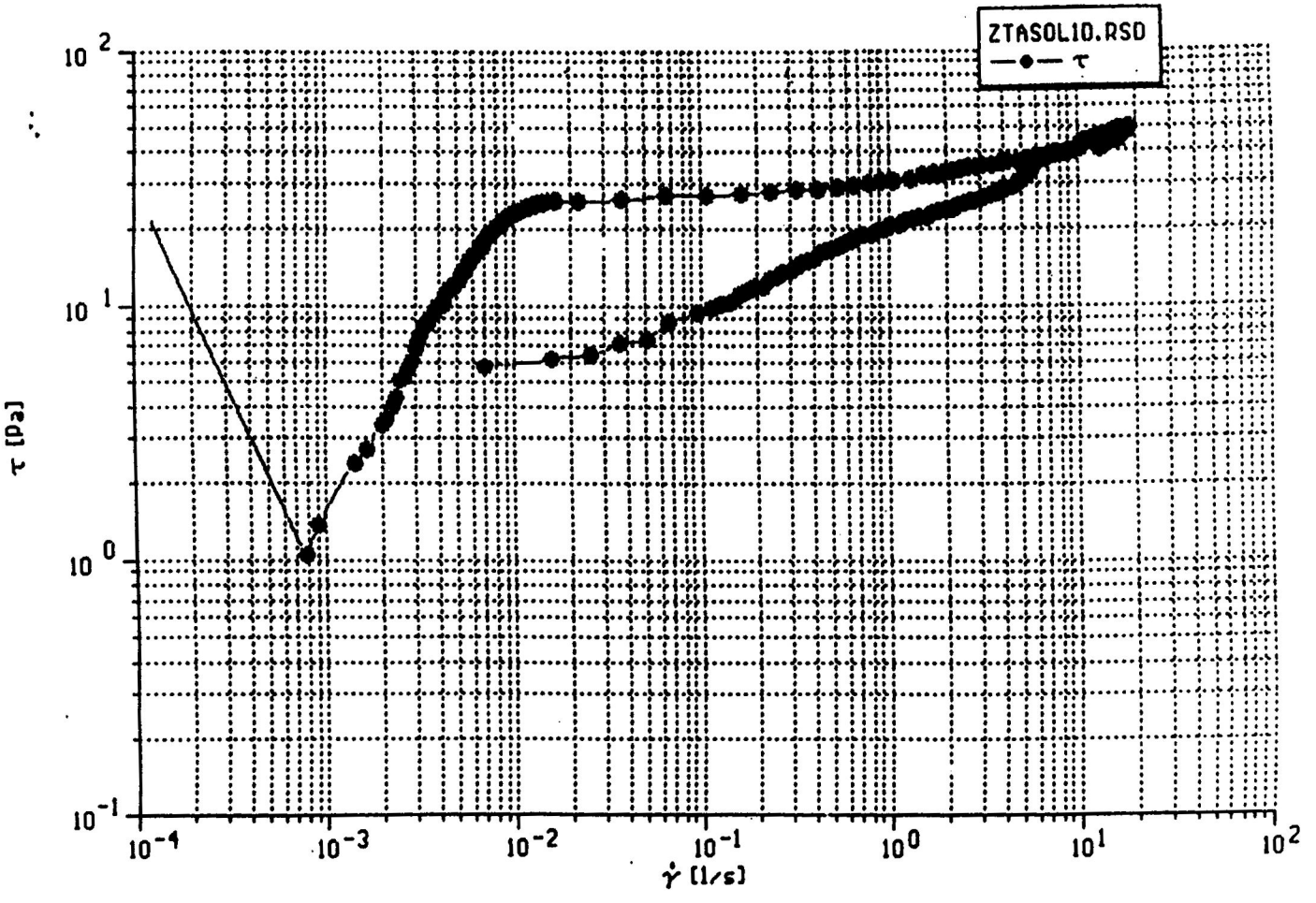

Fig.5.10 Plots of shear stress vs. shear rate of ZTA sol #3

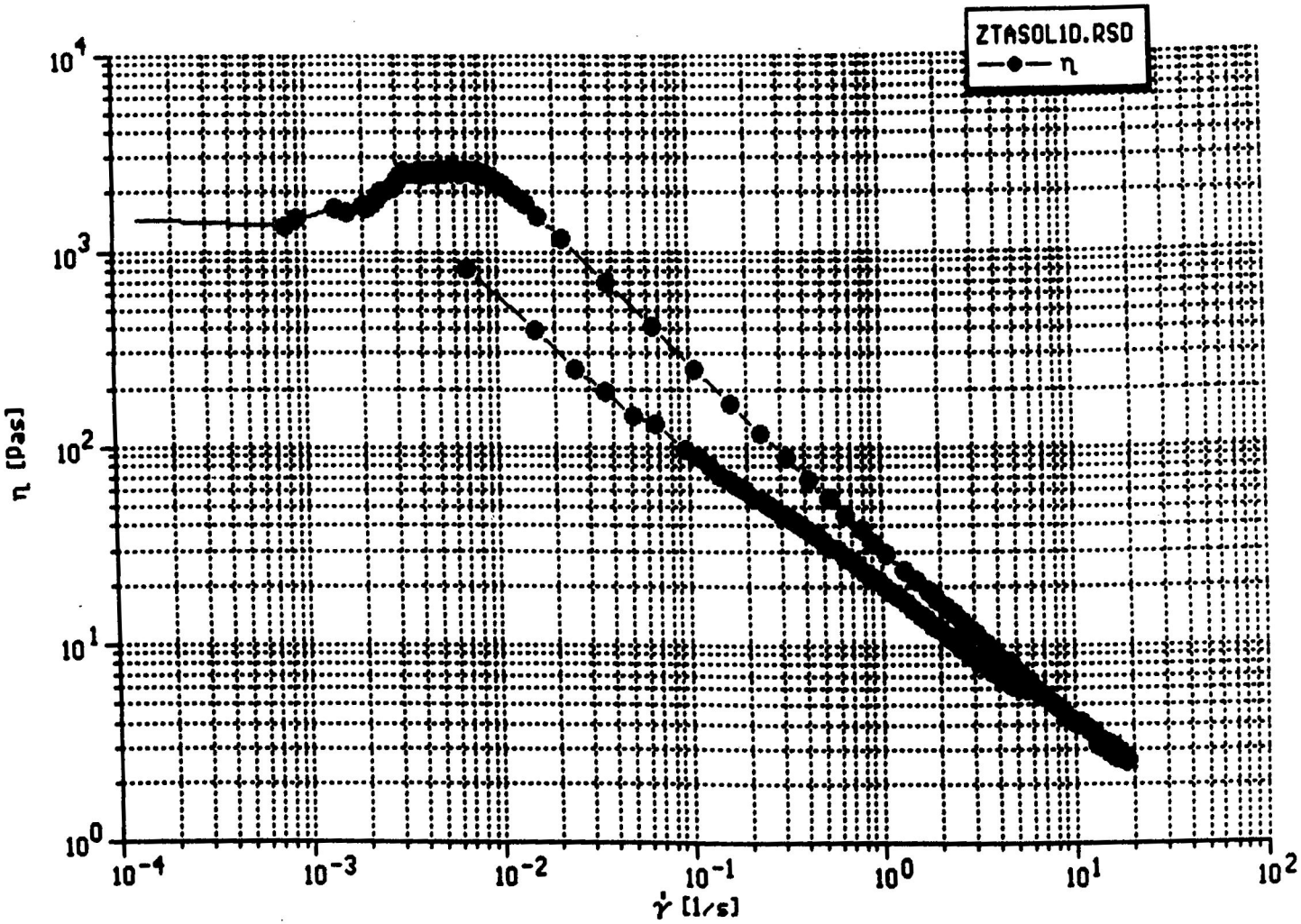

Fig.5.11 Plots of viscosity vs. shear rate of ZTA sol #3

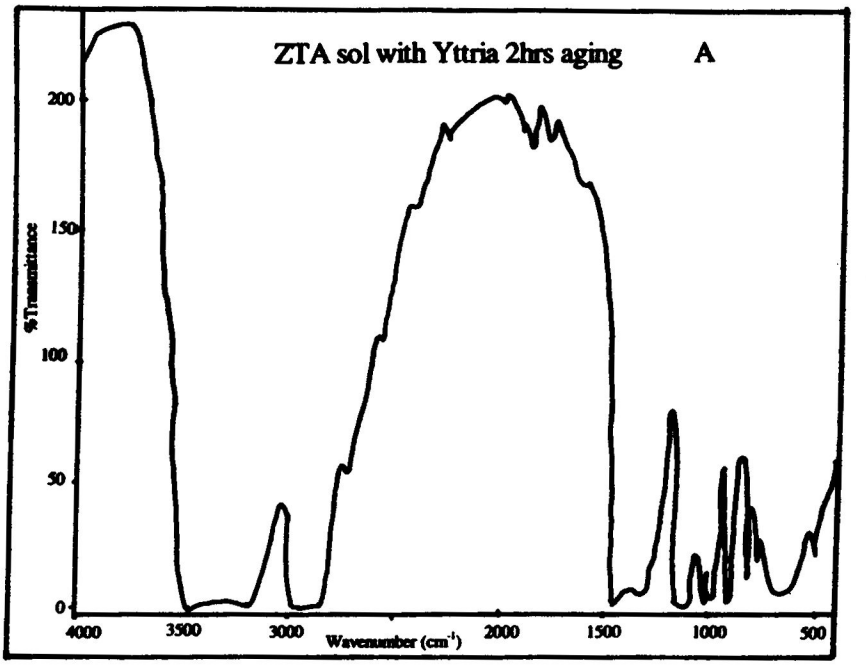

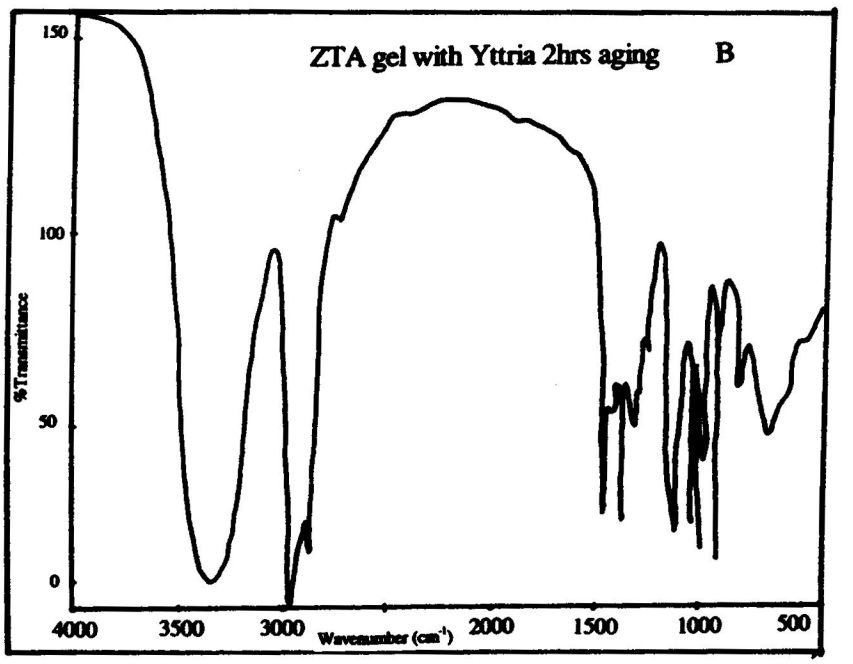

Fig.5.12 FTIR of ZTA sol and gel

consistent with the further extent of reactions and the build-up of structure in the gels as compared to the sols. Fig.5.13 show the FTIR spectra of a ZTA sol with and without yttria after 2hours aging. Fig.5.13A sol and Fig.5.13B sol are the same composition except YIP, because the concentration of YIP is low, so the FTIR of sol A and sol B is almost same.

5.5.2 FTIR of powder

The chemical structures of the samples of powder are revealed by FTIR spectra as shown in Fig5.14. The absorption bands around 3450cm^{-1} are caused by the stretching vibration of -O-H bonds, with increasing heat treatment, a single C bond diminishes at 1000 cm^{-1} in size and a double C bond at 1650 cm^{-1}. The intensity of the bands decreases with increasing temperature, suggesting gradual evaporation of the residual organic compounds, The absorption band 500 cm^{-1} corresponds to the inorganic metal characteristic peak in the sol-gel ZTA powder. The broad absorption band at 530 cm^{-1} corresponds to the characteristic peaks of Al-O. 500 cm^{-1} is broad and appears to include Zr-O peak in the region; The breadth of 500 cm^{-1} narrows with increasing heat treatment temperature. The sharper peak indicates strengthening of the bonds. In the same frequency range, the sharp peak suggests an increase in crystallization.

At 1068, 883, 623 cm^{-1} peaks resulting from the vibration of Al-OH bonds, and at 1660 cm^{-1} for the vibration of H_2O are observed. When the sample is calcined at 1100^{0}C, these absorption peaks disappear. There is a peak appearing at 612cm^{-1}. This absorption

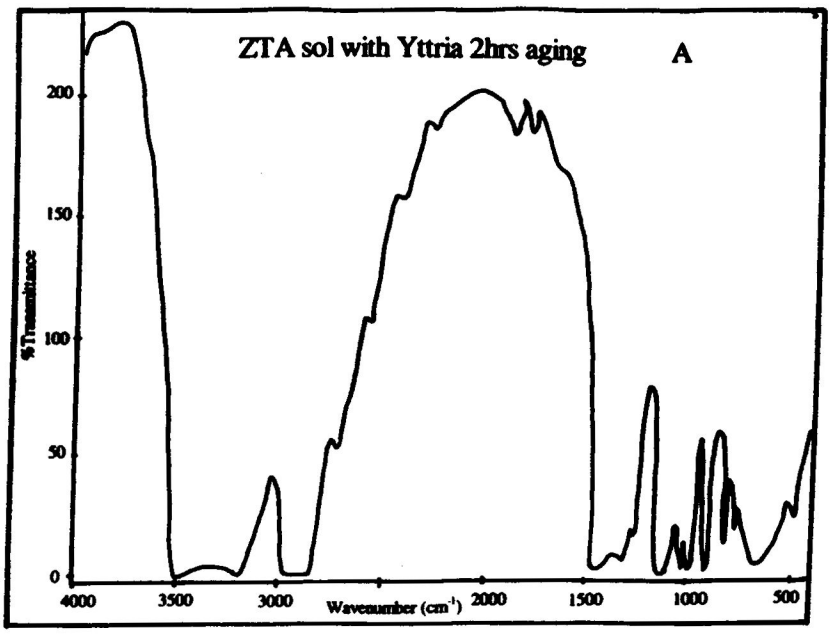

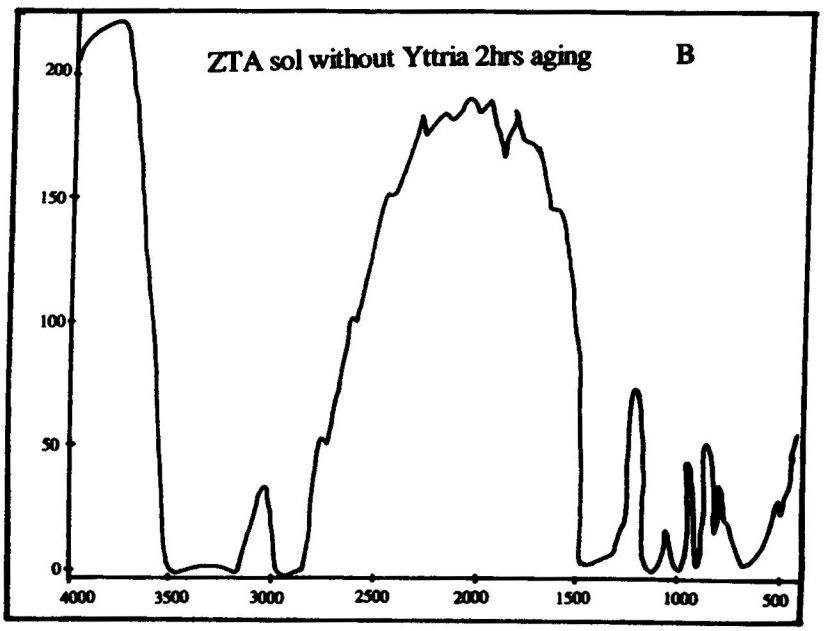

Fig.5.13 FTIR of ZTA sol with and without yttria

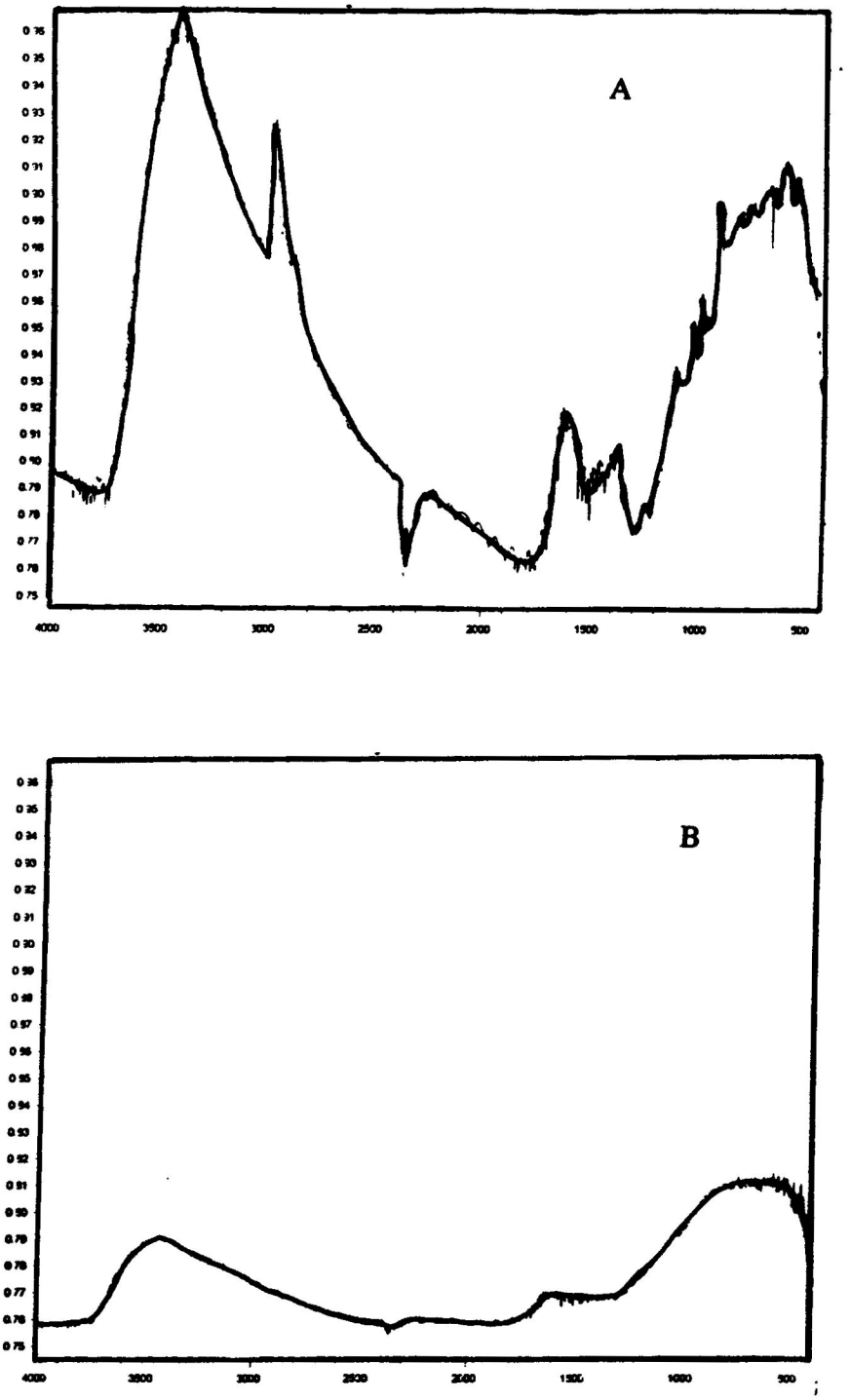

Fig.5.14 FTIR of ZTA powder Al_2O_3=78%, ZrO_2=22%
(A) calcined at 300^{0}C (B) calcined at 600^{0}C

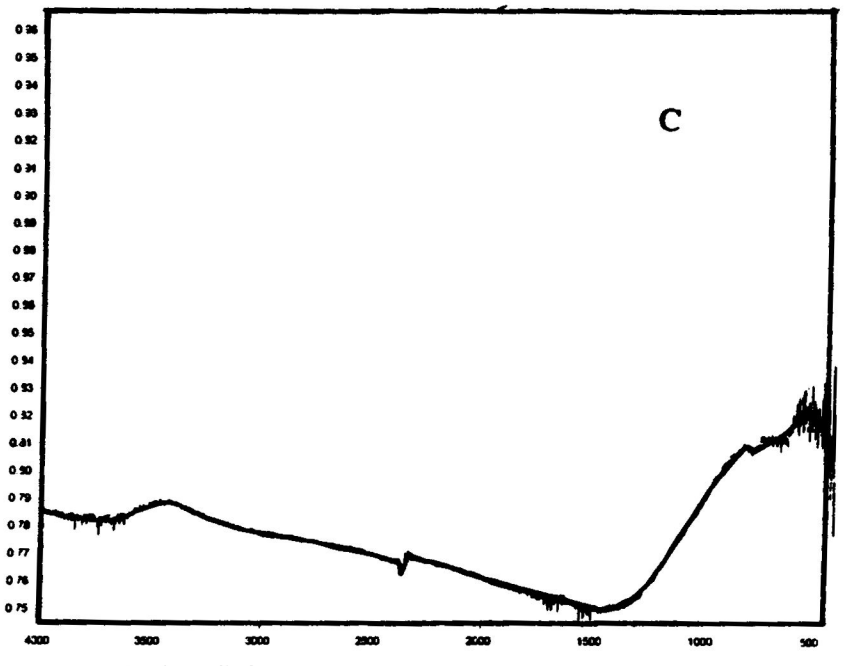

Fig.5.14 FTIR of ZTA powder Al2O3=78%, ZrO2=22%
(C) calcined at 1100^{0}C

peak results from the vibration of Al-O tetrahedral bonds. For the different concentrations of zirconia in the alumina structure, the positions of all peaks have no apparent change, however, the intensities of the peaks are changed. We also find the positions of all peaks show no change in the FTIR spectrum with or without yttria as shown in Fig.5.15.

It should be noted that the absorption peaks of Zr-O vibration, i.e., at 737, 583, and 529 cm^{-1} are not present in the alumina-zirconia powders, the Y-O vibration are not present either. This is possibly due to the stronger intensity of Al-O vibration than that of Zr-O and Y-O vibration. Thereby, the peaks of Zr-O and Y-O vibration are masked.

Some absorption peaks disappear at the calcination temperature of 1100^0C, the other absorption peak appear again at 612 cm^{-1}, which are Al-O tetragonal bonds, and at 580 cm^{-1}, which is an Al-O octahedral vibration band. From the results of FTIR, we conclude that the zirconia and yttria are dispersed in the alumina matrix.

5.6 X-ray Powder Diffraction

5.6.1 X-ray diffraction with different heated temperature

The XRD spectra of an Al_2O_3-ZrO_2 gel are shown in Fig.5.16. At 300^0C the gel remains amorphous. It gives two very broad reflections centred at approximatly 31^0,56^0 (2θ, Cu Kα radiation). The first peak at 31^0 has a larger shoulder at high 2θ angles. These reflections are considered to arise from the rudimentary structure of the gel. When the powder was heated at 900^0C Fig.5.17. the four X-ray diffraction peaks, at 29^0 , 52^0, 60^0, 68^0. XRD spectra show that the glassy state of ZTA powder remains with heating to 900^0C, although some changes in XRD peak intensities occur. Crystalline ZrO_2 appears at

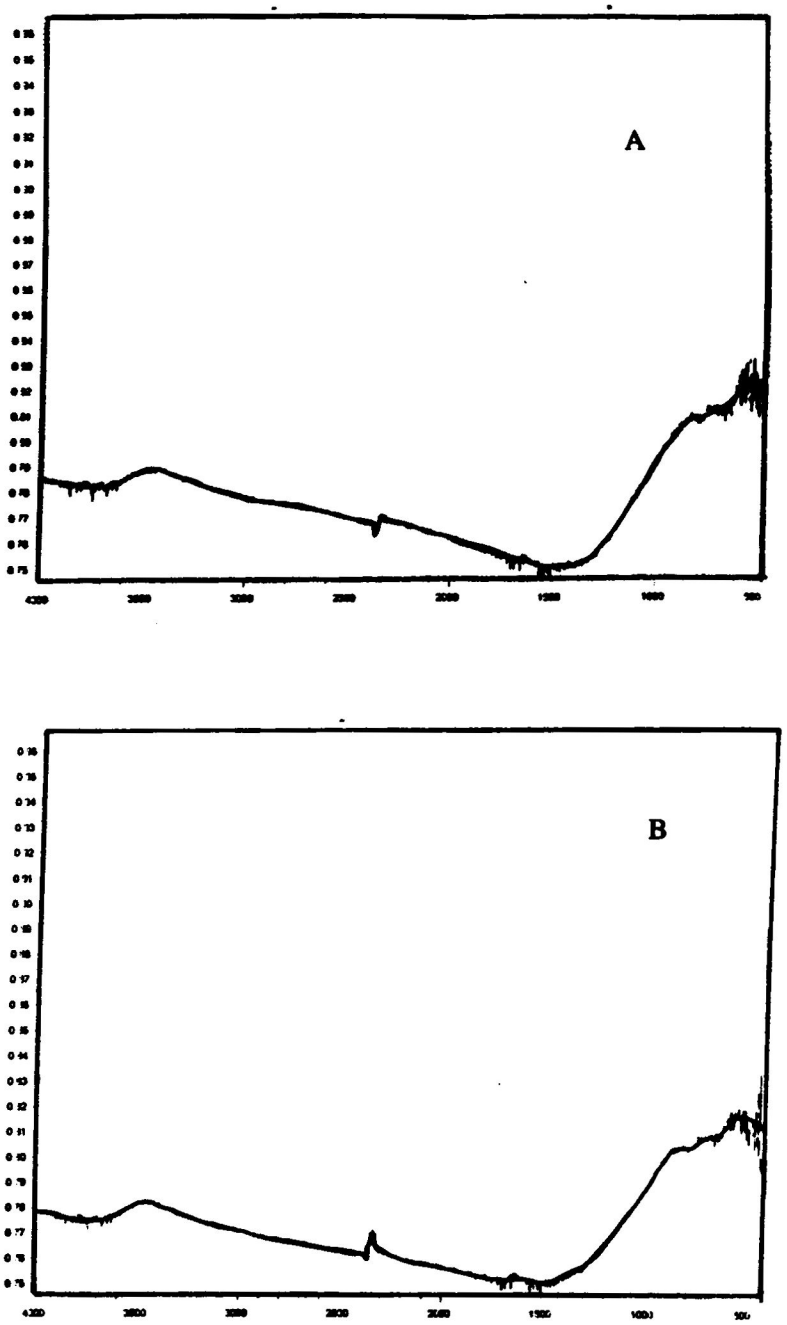

Fig.5.15 FTIR of ZTA powder calcined at 1100^{0}C
(A) Al_2O_3=78%, ZrO_2=22%
(B) Al_2O_3=78%, ZrO_2=22%
Y_2O_3=6 mol% of ZrO_2

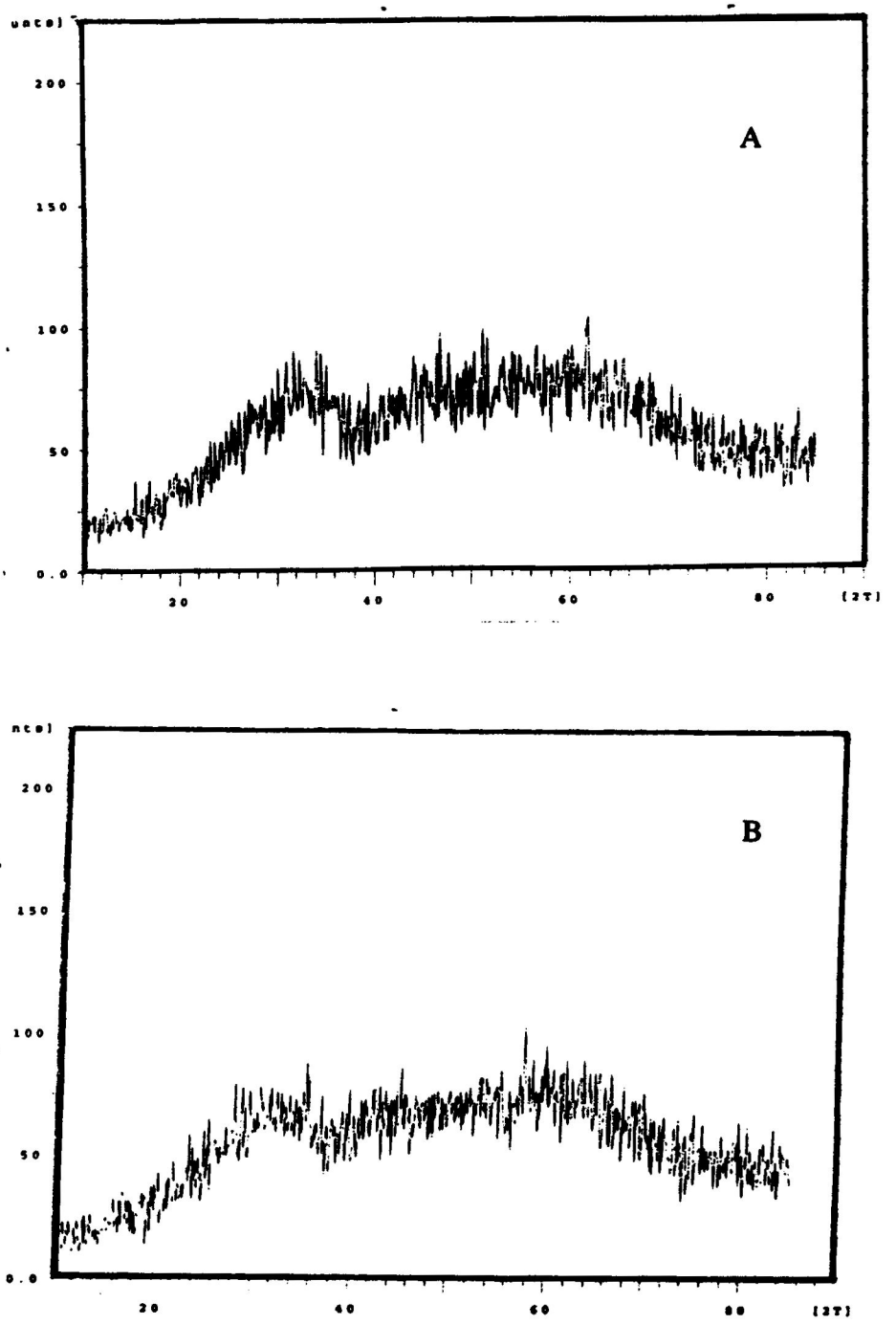

Fig.5.16 X-ray of ZTA powder calcined at 300^{0}C
(A) Al_2O_3=78%, ZrO_2=22%
(B) Al_2O_3=78%, ZrO_2=22%,
Y_2O_3=6 mol% of ZrO_2

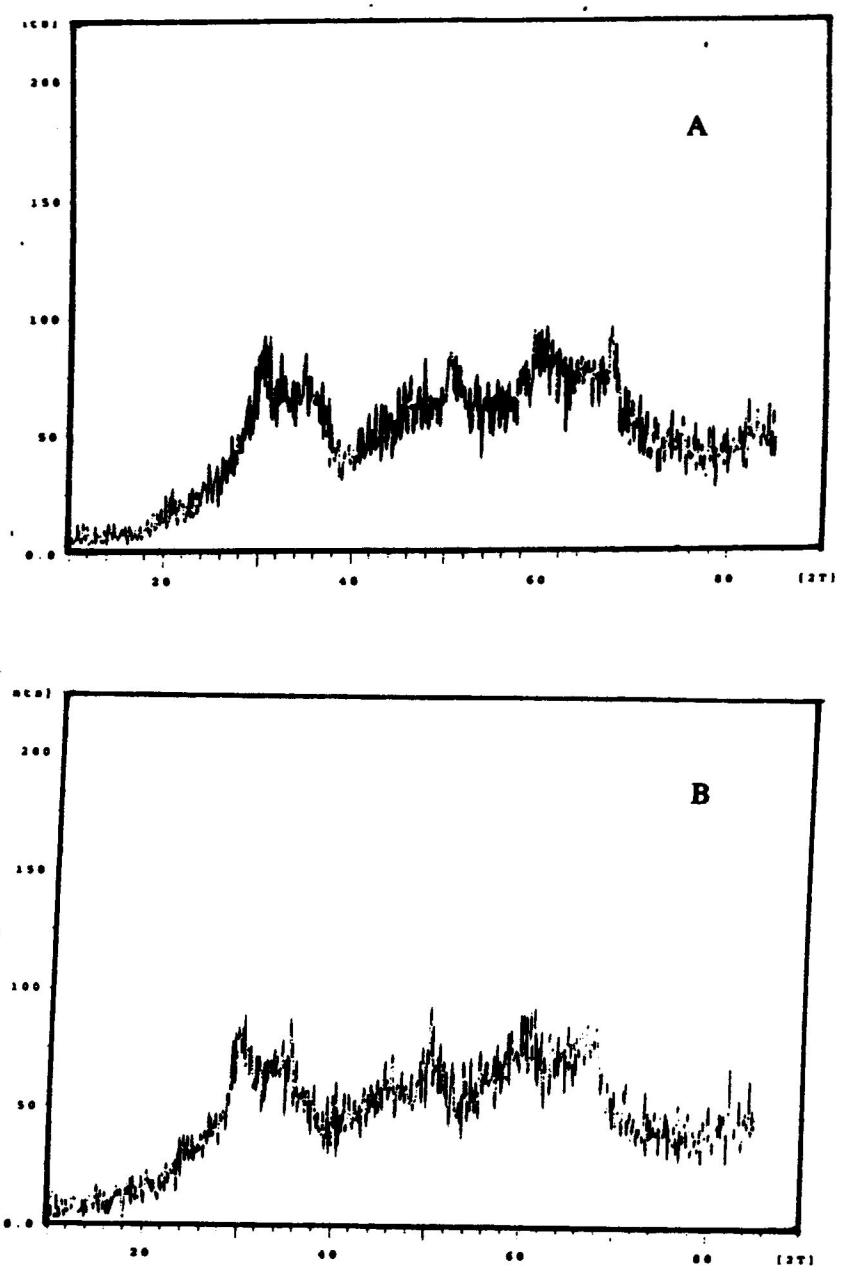

Fig. 5.17 X-ray of ZTA powder calcined at 900°C
(A) Al_2O_3=78%, ZrO_2=22%
(B) Al_2O_3=78%, ZrO_2=22%
Y_2O_3=6 mol% of ZrO_2

900^0C and initially the crystallite diffractions are very broad because the crystallites are small. Their nucleation must be inhomogeneous because the X-rays pattern is still amorphous. The symmetry of the first-formed crystals is apparently cubic(c), thus preserving the cubic-like proto-structure of the gel. This similarity, supported by X-ray diffraction has been widely used as an indicator of apparent c symmetry(41,42).Upon continued heating to 1100^0C, the crystalline component transforms to tetragonal (t) symmetry.

At 1200^0C, The α–Al_2O_3 and t-ZrO_2 crystal phase are completely formed in Fig.5.18. Growth of ZrO_2 crystallites at elevated temperatures was strongly inhibited by Al_2O_3 derived from ASTB. The monoclinic -to-tetragonal phase transformation temperature was lowered in the mixture containing Al_2O_3, and the tetragonal phase was retained on cooling to room temperature. Phase stability is also controlled by particle size since extremely fine particles of ZrO_2 are stable in their tetragonal or even cubic structure at laboratory temperatures(43). This stabilization is a consequence of differences of surface free energies between phases. Strain energy and kinetics may also make some contribution to this phase transformation, but they can be neglected for a purely sol-gel derived powder because of the absence of a rigid matrix.

5.6.2. Effect of ZrO_2 on Crystallization of Al_2O_3

Crystallization depends strongly on the composition of the gel (Al/Zr ratio): the higher the Al/Zr ratio, the higher the temperature at which crystallization occurs.At the

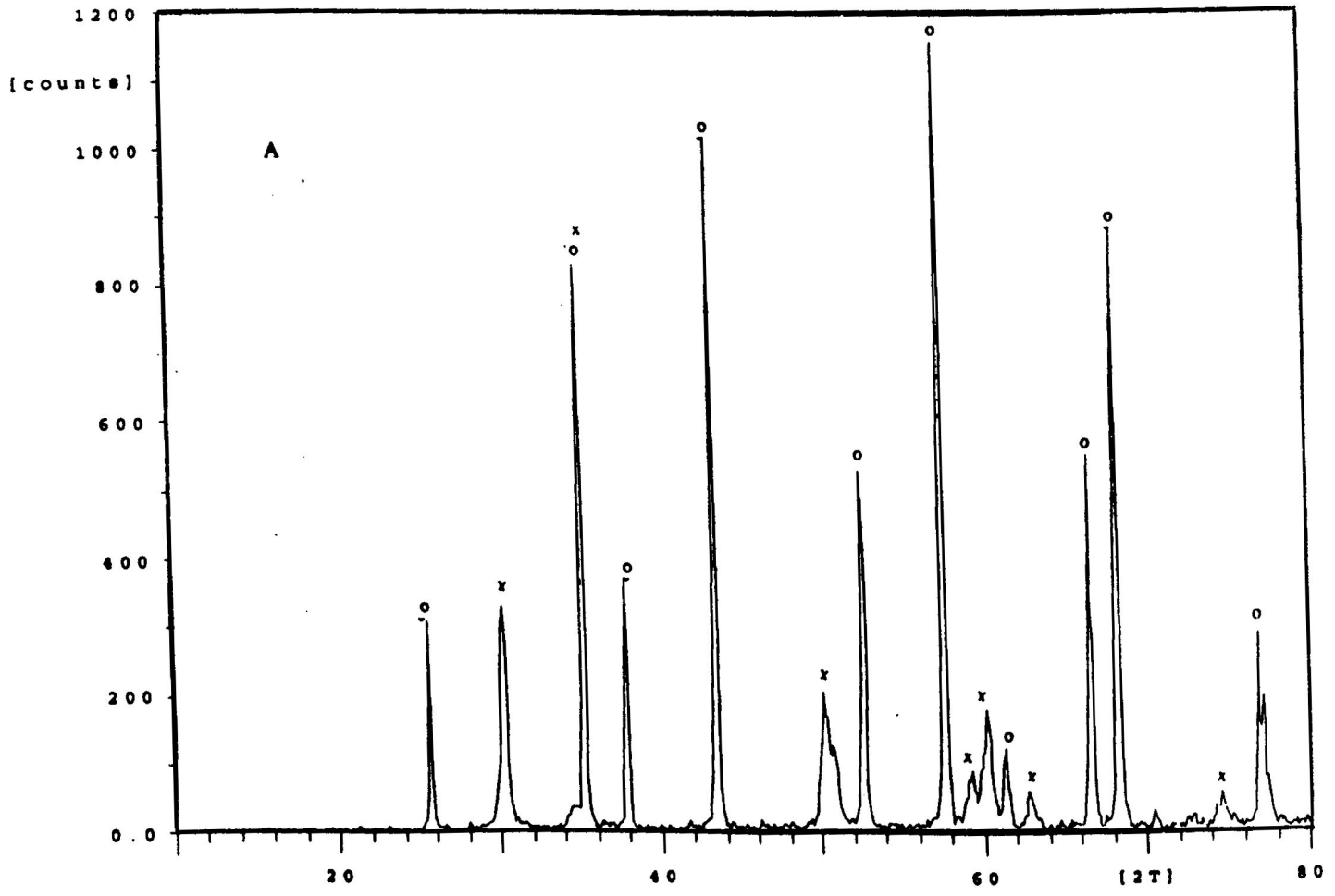

Fig. 5.18A X-ray of ZTA powder calcined at 1200^{0}C
Al_2O_3: 93%, ZrO_2: 7%
x: t-ZrO_2, o: α-Al_2O_3

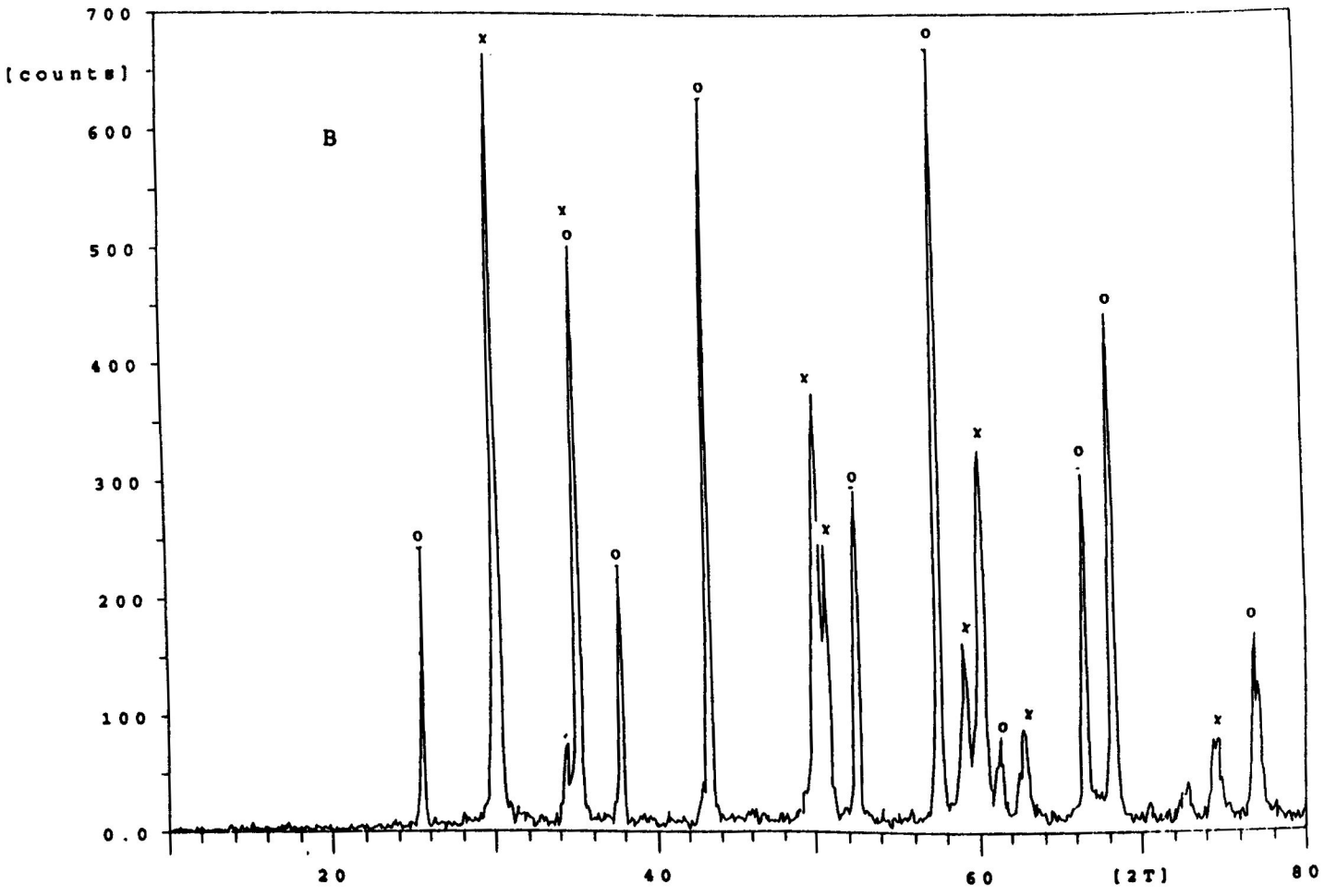

Fig.5.18B X-ray of ZTA powder calcined at 1200^{0}C
Al_2O_3: 85%, ZrO_2: 15%
x: t-ZrO_2, o: α-Al_2O_3

same temperature of 1100^{0}C, XRD spectra show that ZrO_2 is the first phase to nucleate and crystallize; Al_2O_3 needs a higher temperature to crystallize than ZrO_2. Thus, by XRD, the first weak γ-alumina reflections appear around 1100^{0}C in Fig.5.19, the intensity is very weak. But transformation to the stable polymorph (α-alumina) is completed at 1200^{0}C (Fig.5.18.) XRD spectra show that as the content of ZrO_2 increase from 7 volume % (Fig. 5.18A) to 15 % (Fig.5.18B) at same temperature of 1200^{0}C, the crystal intensity is increased.

5.7. Thermal Analysis

The thermal characteristics were examined by thermal gravimetric analysis (TGA) and differential thermal analysis (DTA), The samples used for TGA and DTA experiments were the dried gel. For both DTA and TGA experiments, the samples were heated in a flowing air atmosphere at a heating rate of 10^{0}C/min. The TGA and DTA profiles of the ZTA dried gel powders are shown in Fig.5.19 which shows about 50% total weight loss for samples prepared by sol-gel processing. The weight loss of sol-gel powders as a function of temperature is shown in Fig5.20. The weight loss at 90^{0}C is evaporation of H_2O, the very large weight loss between 200 and 580^{0}C can be attributed to burnout of organics. The sol-gel powder contains a large amount of organics due to the presence of residual organic solvent and residual alkoxy groups bound to aluminum and zirconium and yttrium atoms. There is another exothermic peak which results from the crystallization of γ-alumina. The third exothermic peak is the result which came from γ-alumina transition to

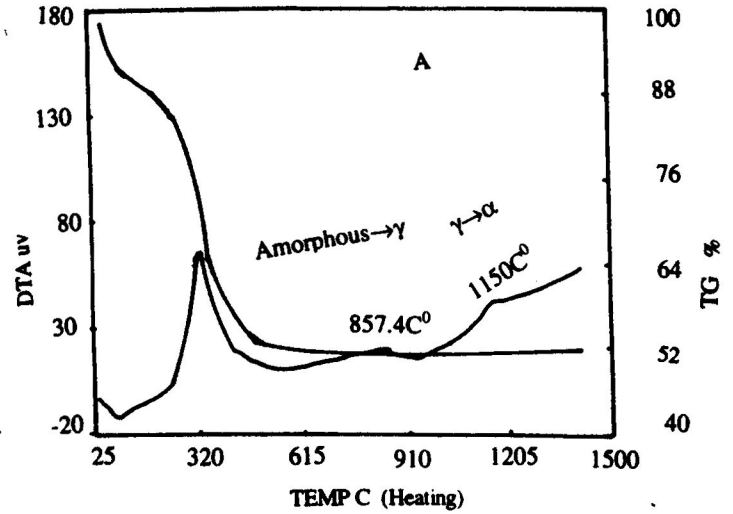

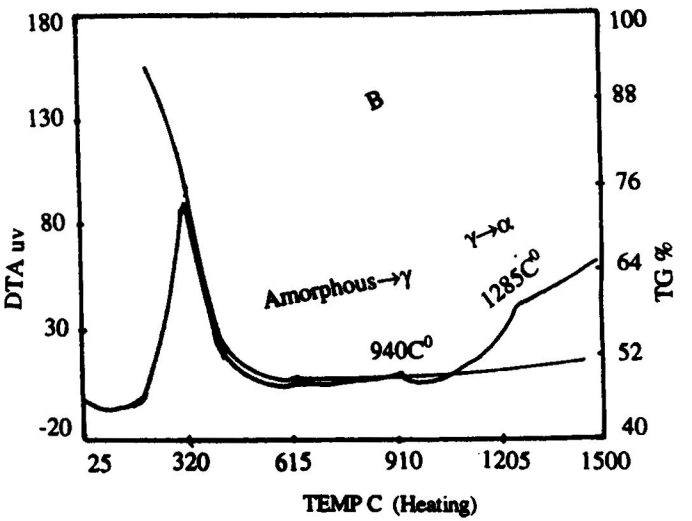

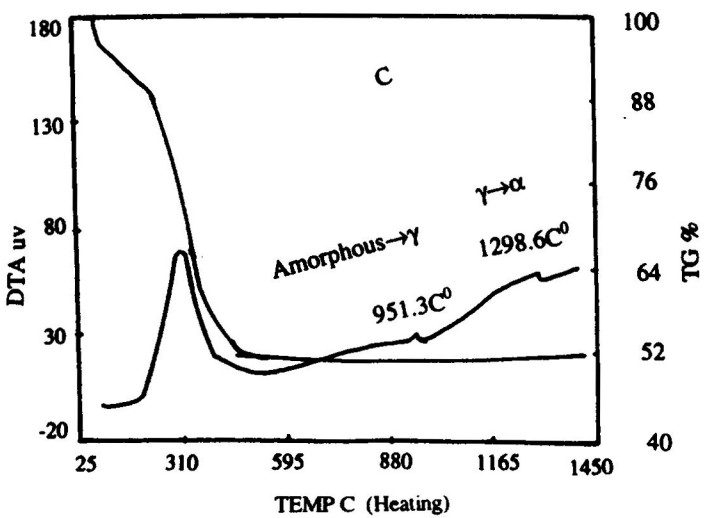

Fig.5.19 DTA and TGA curves
(A) Alumina gel
(B) ZTA gel, ZrO_2 = 7%
(C) ZTA gel, ZrO_2 = 15%

α-alumina. From Fig.5.20(B), 5.20(C), in the presence of zirconia, the Alumina phase transformation takes place at a considerably higher temperature than in pure alumina, the alumina phase transformation in powder compacts is shifted from 1150^0C to 1270^0C(7% ZrO_2) and to 1298^0C(15% ZrO_2), The more volume percent of ZrO_2. the greater the shift to higher transformation temperature.

CHAPTER 6

CONCLUSIONS

Based on the results and discussion in chapter v, the following conclusions can be drawn:

A preparation process for ZTA powders by the sol-gel method was successfully used. Transparent gels could be produced from ATSB, ZRP, YIP using triethanolamine as a chemical modifier for the alkoxides. The modified precursor appears quite attractive for the preparation of multicomponent systems. The presence of poorly hydrolyzable ligands showed down the hydrolysis condensation process. Condensation reactions with other precursors can take place during the gelation. In this sol-gel process, the TEA/alkoxide molar ratio plays an important role in the time for gel-formation. The influence of the chelating agent on the particle formation manifests itself as the reduction of the number of available condensation sites.It is possible to obtain homogeneous gels on a molecular scale using chelated alkoxides. From the XRD diagram, the transition γ-alumina$\rightarrow$ α-alumina takes place at a lower temperature with the powder preparation from sol-gel method .

Alumina is completely transformed into the α phase after calcination at 1200^{0}C. The tetragonal phase was retained on cooliong to room temperature in the mixture containing Al_2O_3. From the TG/DTA curves, in the presence of zirconuim, the alumina phase transformation takes place at a higher temperature than in pure alumina, the more volume percent of ZrO2, the more shift of transformation temperature.The ZrO_2-Al_2O_3 powders obtained by the sol-gel technique are fine and contain t-ZrO_2; they thereby appear to be adequate for the investigation on the mechanism of stability of t-ZrO_2. The total amount of water for hydrolysis has an effect on particle size. The rate of hydrolysis depends on the nature of both the metal ions and the alkoxide groups. The results show that the particle size increases with increasing zirconia content and calcination temperature.

References

1. N.Claussen, *J. Am. Ceram. Soc.*, 59[1-2] 49-51 (**1976**).

2. N. Claussen, J. Steeb, and R.F. Pabst, *Am Cer. Soc.* Bull., 56[6]559-62(**1977**).

3. P.F. Becher, *J. Am. Ceram. Soc.*,64[1]37-39(**1981**).

4. H. Kamiya, M. Takatau, and A. Hattori., *J. Ceram.* Jpn. 98[5]456-63(**1990**).

5. H.Kamiya and M. Takatsu, *J. Ceram. Soc.* Jpn. 98[1]13-21(**1990**).5. A. G. Evans and K.T.Faber, *J.Am. Ceram. Soc.*, 64[7]394-98(**1981**).

6. J.G. Duh and M.Y. Lee, *J.Mater. Sci.* 24, 4467 (**1987**).6. R. McMeecking and A. G. Evans, *J. AM. Ceram. Soc.*, 65[5]242-46(**1982**).

7. B.E. Yoldas, *J. Am. Ceram. Soc.* 65,387 (**1982**).

8. A. H. Heuer, *J. Am. Ceram. Soc.* 70, 689 (**1987**).

9. E.c. Subba Rao, in Advances in Ceramics (*The American Ceramic Society*, Westerville, OH, **1981**), Vol.3.

10. R. C. Garvie, R. H. Hannink, and R. T. Pascoe, *Nature* 258, 703 (**1975**).

11. D. L. Porter and A. H. Heuer, *J.Am. Ceram. Soc.* 60,183 (**1977**).

12. L. L. Fehrenbacher, L. A. Jacobson, and C. T. Lynch, in Rare Earth ResearchIII10. R. C. Garvie, R.H.Hannink, and R. T. Pascoe, *Nature* 258, 703 (**1975**)

13. V. S. Nagarajan and K.J. Rao, *J. Mater. Sci.* 24, 2140 (**1989**).

14. R. C. Garvie, in *Adv. Ceram.* 24, 55 (**1988**).

15. H. Schubert and G. Petzow, in *Adv. Ceram.* 24, 21 (**1988**).

16. A. H. Heuer, N. Claussen, W. M. Kriven, and M. Ruhle, *J. Am. Ceram. Soc.* 65, 642 (**1982**)

17. M. Yoshimura, *Ceram. Bull.* 67, 1950 (**1988**).

18. J. Livage, K. Doi, and C. Mazieres, *J. Am. Ceram. Soc.* 51, 349 (**1968**).

19. K. S. Mazdiyasni, C. T. Lynch, and J. S. Smith, *J. Am. Ceram. Soc.* 49, 283 (**1966**).

20. R. C. Garvie, *J. Phys. Chem.* 69, 1238 (**1965**).

21. E. Tani, M. Yoshimura, and S. Somiya, *J. Am. Ceram. Soc.* 66, 11 (**1983**).

22. T. Itoh, *J. Mater. Sci.* Lett. 4, 1029 (**1985**).

23. R. P. Denkewicz, Jr.,k.S. TenHuisen, and J. H. Adair, *J. Mater. Res.* 5, 2698 (**1990**).

24 C. Hu and M. Rahaman, *J. Am. Ceram. Soc.* 77[3]815-19(**1994**).

25. K. Ranjbar b. Rao, and T. Mohan, *Am. Cer. Soc. Bull.* 73[2]63-66(**1994**)

26 P. Homerin, F. Thevenot. G. Orange, G. Fantozzi, V. Vandeneede, A. Leriche and F. Cambier, *J. Phs.* (Paris), Colloq. C1, 2 (**1986**) C1-717.

27. A. Leriche, G. Mortgaat, F. Cambier, P. Homerin, F. Thevenot, G. Orange and G. Fantozzi, *Science and Technology of Zirconia III*, Tokyo, 9-11 September **1986**, in press

28. P. Homerin, Preparation et caracterisation de materiaux ceramiques a base d'alumine renforce par une dispersion de zircone, These, Ecole des Mines de Saint-Etinne, **1987** No. 87 ISAL 0041.

29. J. P. Bach, P. Homerin, F. Thevenot, G. Orange and G. Fantozzi, in P. Vincenzini (ed), Proc. World Congress on High Technology Ceramics, 6th CIMTEC, Milan, June **1986**, Elsevier, Amsterdam.

30. J. P. Bach, Elaboration et caracterisation de composites alumine-zircone prepares a partir de differents precurseurs, These, Ecole des Mines de Saint-Etienne, 1988, No 16TD, p. 216.

31. J. P. Bach, F.Thevenot, G. Orange, G. Fantozzi and P. Vergnon, Silicates Ind., 53(9-10) (**1988**) 153-156

32. H. Kamiya, M. Sakakibara, Y. Sakurai and G. Jimbo, *J. Am. Ceram.*

33. J. P. Bach, F.Thevenot, B. Mirhadi and H. Hausner, Rev. Hautes Temp. Refract., 24(**1987**) 211-217

34. J. P. Bach, P. Orlans, J. P. Lecompte, B. Guihot and F. Thevenot, in D. Taylor (ed.), Proceeding of Science of Ceramics 14, Canterbury, U. K., September 1987, *Institute of Ceramics*, Shelton, Staffs., **1988**, pp. 175-180.

35. J.C. Pouxviel, J.P. Boilot, J.C. Beloeil and J.y. Lallemann, J. Non-Cryst. Solids 89 (**1987**) 345

36. J.C. Pouxviel, J.P. Boilot, A. Dauger and A. Wright, *J. Non-Cryst. Solids* 103 (**1988**) 331

37. J.C. Pouxviel and J.P. Boilot, *J. Mater. Sci.* 24 (**1989**) 321.

38. F. Chaput, J. P. Boilot, A. Dauger, F. Devreux and A. DeGeyer, *J. Non-Cryst. Solids* 116 (**1990**) 133

39. T.Heinrich and F. Raether, *J. Non-Cryst. Solids* 147&148 (**1992**) 152

40. T. Heinrich, F. Raether, O. Spormann and J. Fricke, *J. Appl. Crystallogr.* 24 (**1991**) 788

41. T. Heinrich, F. RAether, W. Tappert and J. Fricker, *J. Non-Cryst. Solids* 145 (**1992**)